Electronic Supplementary Material (ESI) for ChemComm.


# Synthesis and investigation of a *meta*[6]cycloparaphenylene gold(I) *N*-heterocyclic carbene complex

Felix Bernt, Christopher M. Leonhardt, Dominic Schatz, and Prof. Dr. Hermann A. Wegner*

*Institute of Organic Chemistry, Justus Liebig University Giessen, 35392 Giessen, Germany*

*Centre for Materials Research (ZfM/LaMa), Justus Liebig University Giessen, 35392 Giessen, Germany*

E-mail: hermann.a.wegner@org.chemie.uni-giessen.de

## Table of Contents

# 1. General Information

**Reagents and solvents:** In case of no further descriptions, all chemicals were used as received from commercial manufacturers (Acros Organics, Sigma Aldrich, TCI, BLD Pharm, and others). All chemical reactions were done under inert gas atmosphere in dried vessels using Schlenk-technique if not stated otherwise. Technical grade solvents used during work-up and purification were distilled prior to use.

**$^{1}$H-NMR spectroscopy:** Proton-Nuclear Magnetic Resonance ($^{1}$H-NMR) spectra were measured on a Bruker Avance II 400 (400 MHz), Avance III 400 MHz HD (400 MHz), Avance 600 (600 MHz) or Avance Neo 700 (700 MHz). All measurements were performed at 295 K. Chemical shifts ($\delta$) are reported in parts per million (ppm) relative to residual solvent signals or tetramethylsilane (TMS), while coupling constants ($J$) are reported in Hertz (Hz). Multiplicities are abbreviated as s (singlet), d (doublet), t (triplet), and m (multiplet). Assignments are given as $XH_{\#}$, where X is the number of equivalent protons and # is the number of the correponding positions.

**$^{13}$C-NMR spectroscopy:** Carbon-Nuclear Magnetic Resonance ($^{13}$C-NMR) spectra were measured on a Bruker Avance 400 (101 MHz), Avance III 400 MHz HD (101 MHz), Avance 600 (151 MHz) or Avance Neo 700 (176 MHz). All measurements were performed at 295 K. Chemical shifts ($\delta$) are reported in parts per million (ppm) relative to residual solvent signals or tetramethylsilane (TMS). Assignments are given as $XC_{\#}$, where X is the number of equivalent carbons and # is the number of the correponding positions.

**High-resolution mass spectrometry:** ESI-MS spectra were measured on a Bruker Daltonics Micro TOF LC. The samples were dissolved in methanol. A positive voltage of 4500 V was applied to the capillary and -500 V to the End Plate Offset. The nebulizer was set to 0.4 bar. The dry heater was set to 180 °C and the flow of nitrogen as the dry gas to 4.0 L/min.

APCI-MS spectra were measured on a Bruker Daltonics Micro TOF LC. The samples were dissolved in methanol. A positive voltage of 1500 V was applied to the capillary and -500 V to the End Plate Offset. The nebulizer was set to 2.5 bar. The dry heater was set to 200 °C and the flow of nitrogen as the dry gas to 3.0 L/min.

**Infra-red spectroscopy:** IR spectra were measured on a Bruker ALPHA IR-spectrometer. For the measurements the attenuated total reflection (ATR) methodology was applied. The intensities are abbreviated as w (weak), m (medium), and s (strong).

**Column chromatography:** For column chromatography, Silica gel 60 (0.04 – 0.063 mm) from Macherey-Nagel GmbH & Co. was used.

**Melting points:** Melting points were determined on a M5000 melting point meter from A. KRÜSS Optronic GmbH, Germany. A heating rate of 1 °C min$^{-1}$, a resolution of 0.1 °C were used, with a measurement accuracy of ±0.3 °C (25 – 200 °C), and ±0.5 °C (200 – 400 °C).

**UV-vis spectroscopy:** SPECORD® 200 PLUS UV-vis spectrophotometer equipped with two automatic eightfold cell changers and a Peltier thermostat system for temperature control manufactured by Analytic Jena was used. The spectrophotometer system is operated by the software ASpect UV from Analytic Jena.

**Fluorescence spectroscopy:** For fluorescence and excitation spectra a FP-8300 spectrofluorometer (Jasco), was used. For fluorescence spectra, the samples were irradiated with light with the excitation wavelength of the corresponding absorption maximum and a bandwidth of 2.5 nm. The scanning speed was set to 200 nm/min and the data interval to 0.2 nm. For excitation spectra, the samples were irradiated with light with the excitation wavelength of the two corresponding emission maxima. The other parameters were set the same as for the fluorescence spectra. All samples were measured in QS High Precision Cells made of Quartz Suprasi® (Hellma Analytics) with a light path of 10 mm.

**Crystallographic data:** Suitable single crystals for X-ray structure determination were selected and transferred in protective perfluoropolyether oil on a microscope slide. The selected and mounted crystals were transferred to

the cold gas stream on the diffractometer. The diffraction data were obtained at 100 K on a Bruker D8 three circle diffractometer, equipped with a PHOTON 100 CMOS detector and a IμS microfocus sources with Quazar mirror optics (Mo-Kα radiation, $\lambda$ = 0.71073 Å).
The data obtained were integrated with SAINT and a semi-empirical absorption correction from equivalents with SADABS-2016/2 was applied.[1] The structures were solved by direct methods using SHELXT-2018/2.[2] Structure refinement was done using SHELXL-2018/3.[3] All non-hydrogen atoms were refined anisotropically and C-H hydrogen atoms were positioned at geometrically calculated positions and refined using a riding model. The isotropic displacement parameters of all hydrogen atoms were fixed to 1.2x or 1.5x ($CH_3$ hydrogens) the $U_{eq}$ value of the atoms they are linked to.

**Computational methods:** All density functional theory (DFT) computations were carried out using the ORCA software package.[4,5] The preliminary geometry was obtained from an extended tight binding (XTB) optimization,[6] followed by a conformer screening using the conformer rotamer ensemble sampling tool (CREST).[7,8] The lowest lying conformer was optimized by the means of DFT using the zeroth-order regular approximation (ZORA) at a PBE0/ZORA-def2-TZVP/D3BJ/CPCM($CHCl_3$) level of theory.[9–15] For the gold atom, a separate gaussian type orbital (GTO) was defined using the SARC-ZORA-TZVP basis set.[16] On all atoms, the SARC/J auxiliary basis set was used for the RIJCOSX approximation.[17,18]
Due to a tricky potential energy surface, the Hesse matrix was recalculated at every 5$^{th}$ step of the geometry optimization to reach a geometry with no imaginary vibrational modes, which was verified in a separate frequency calculation on the same level of theory. The electronic transitions were computed using time-dependent DFT (TD-DFT) within the Tamm-Dancoff approximation (TDA)[19] at a PBE0/ZORA-def2-TZVPP/D3BJ/CPCM($CHCl_3$) level of theory with a separate GTO for the gold atom (SARC-ZORA-TZVPP).[9–16] On all atoms, the SARC/J auxiliary basis set was used for the RIJCOSX approximation.[17,18]

**Topographic steric map**: The steric demand of the NHC ligand was analysed by using the web application SambVca2.[20–22] As a result, the buried volume[23] and the steric map[24] were obtained.

# 2. Synthetic Procedures

## ***N*-(Mesityl)-oxanilic acid S1**

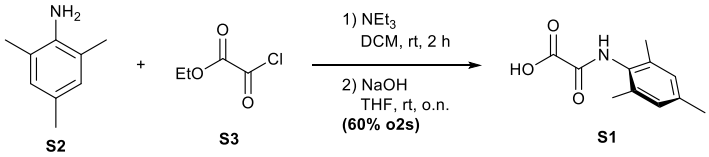


**S2** **S3** **S1**

This compound was synthesized according to literature.[25]
A solution of 2,4,6-trimethylaniline (**S2**) (3.65 mL, 25.1 mmol, 1.00 equiv.) and triethylamine (3.65 mL, 24.9 mmol, 0.994 equiv.) in anhydrous THF (20 mL) was cooled to 0 °C. At this temperature, ethyl chlorooxoacetate (**S3**) (2.80 mL, 25.1 mmol, 1.00 equiv.) was added slowly via syringe. Precipitation of a colourless solid occurred immediately upon addition. The mixture was allowed to stir for 2 h after warming to rt. At this point, the solid was filtered off, and the organic layer was washed with 2 M HCl solution (2x20 mL). The aqueous layer was washed with ethyl acetate, and the combined organic layers were washed with brine (50 mL), and dried over $MgSO_4$. The solvent was then removed under reduced pressure, leaving a pale yellow solid. Recrystallization from hexanes afforded the *N*-(mesityl)-oxanilic acid ethyl ester as colourless solid (4.24 g, 18.0 mmol, 72%).
The *N*-(mesityl)-oxanilic ethyl ester (518 mg, 2.20 mmol, 1.00 equiv.) was subsequently dissolved in THF (10 mL). To this solution was added 1 M NaOH solution (40 mL), and the mixture was stirred overnight at rt. Diethyl ether (20 mL) was added, and the layers were separated. The organic layer was washed with 1 M NaOH solution (20 mL). The aqueous layer was then acidified with 2 M HCl until precipitation occurred. The aqueous phase was then extracted with ethyl acetate (2x20 mL). The ethyl acetate was washed with brine (20 mL), and then dried over $MgSO_4$. Removal of the solvent under reduced pressure provided the *N*-(mesityl)-oxanilic acid (**S1**) as a colourless solid (383 mg, 1.85 mmol, 84%).

**Mp.** = 106 °C.

**$^1$H-NMR** (400 MHz, 297 K, $CDCl_3$): $\delta$ = 8.47 (s, 1H); 6.94 (s, 2H); 2.29 (s, 3H); 2.20 (s, 6H) ppm.

**$^{13}$C-NMR** (101 MHz, 297 K, $CHCl_3$): $\delta$ = 159.80 (1C); 155.97 (1C); 138.57 (1C); 134.65 (2C); 129.45 (2C); 128.85 (1C); 21.11 (1C); 18.41 (2C) ppm.

**HRMS (ESI)** *m/z* calc. for. $C_{11}H_{13}NO_3 + Na^+$: 230.0787 $[M+Na]^+$; found: 230.0788.

## Cyano-*meta*[6]cycloparaphenylene 1

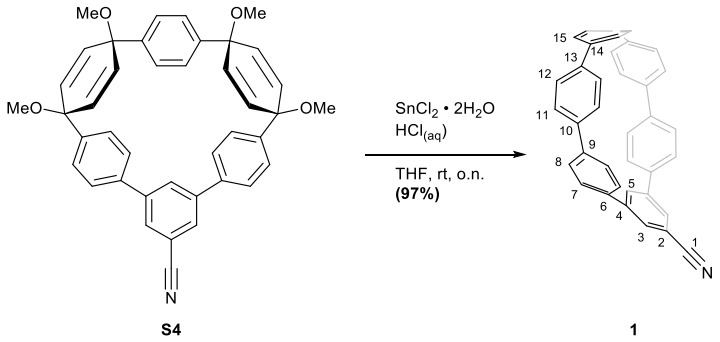


This compound was synthesized according to literature.[26]
$SnCl_2$ x $2H_2O$ (2.46 mg, 10.9 mmol, 8.00 equiv.) was added to a Schlenk-flask together with THF (273 mL), followed by dropwise addition of concentrated HCl (1.82 mL, 21.8 mmol, 16.0 equiv.). This solution was allowed to stir at rt for 30 min.
(*note: if the tin chloride is too old, then the solution becomes cloudy during the addition of HCl, and the reaction does not work properly).*

The freshly prepared $H_2SnCl_4$ solution was added to the macrocyclic precursor **S4** (825 mg, 1.36 mmol, 1.00 equiv.) at rt in a Schlenk tube. After stirring overnight, the reaction was quenched with aqueous $NaHCO_3$ solution (250 mL). The product was extracted with DCM (3x200 mL) and the combined organic layers have been washed with water (3x150 mL) and brine (150 mL). After drying over magnesium sulphate, and subsequent filtration, the volatiles were removed at the rotary evaporator to obtain the crude product. Further purification was done using flash column chromatography ($SiO_2$, Cy/DCM/EtOAc = 6:1:1) to obtain cyano-*meta*[6]cycloparaphenylene **1** (631 mg, 1.32 mmol, 97%).

**Mp.** = >290 °C (slow decomposition)

**$^1$H-NMR** (400 MHz, 297 K, $CD_2Cl_2$): $\delta$ = 7.74 (d, $J$ = 1.85 Hz, $2H_3$); 7.48 – 7.42 (m, $16H_{8,11,12,15}$); 7.15 – 7.12 (m, $4H_7$); 6.04 (t, $J$ = 1.85 Hz, $1H_5$) ppm.

**$^{13}$C-NMR** (101 MHz, 297 K $CD_2Cl_2$): $\delta$ = 144.03 ($1C_5$); 143.83 ($2C_6$); 140.97 (2C); 139.95 (2C); 137.99 (2C); 136.95 (2C); 136.52 (2C); 129.83 ($4C_7$); 128.41 (4C); 128.27 (4C); 128.22 (4C); 127.95 (4C); 126.35 ($2C_3$); 119.41 ($1C_1$); 113.29 ($1C_2$) ppm.

**IR (ATR):** $\tilde{\nu}$ = 3052 (m); 2926 (m); 2225 (m); 1715 (w); 1577 (s); 1482 (s) $cm^{-1}$.

**HRMS (ESI)** *m/z* calc. for $C_{37}H_{23}N + Na^+$: 504.1722 $[M+Na]^+$; found: 504.1723.

## Amino-methylene-*meta*[6]cycloparaphenylene 2

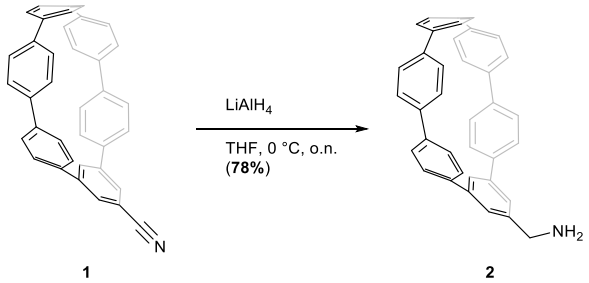


1 2

This compound was synthesized according to a modified literature procedure.[26]
In a Schlenk flask $LiAlH_4$ (52.5 mg, 1.24 µmol, 3.00 equiv.) was added in small portions to a solution of cyano-*meta*[6]cycloparaphenylene **1** (200 mg, 415 µmol, 1.00 equiv.) in THF (10 mL) at 0 °C. The resulting mixture was allowed to warm up to rt and stirred overnight. The next day, a saturated solution of sodium/potassium tartrate (150 mL) was added and allowed to stir for 1 h at room temperature. After extraction of the aqueous phase using $Et_2O$ (3x100 mL), the combined organic layers were dried over magnesium sulphate, filtered and the volatiles were removed at the rotary evaporator. The crude product was further purified by flash silica gel chromatography ($SiO_2$, DCM/MeOH = 19:1 + 0.5% TEA) to obtain the desired product **2** (157 mg, 323 µmol, 78%)

**Mp.** = slow decomposition >250 °C

**$^1$H-NMR** (400 MHz, 298 K, DCM-$d_2$): $\delta$ = 7.45-7.38 (m, 18H); 7.17 – 7.14 (m, 4H); 5.63 (t, $J$ = 1.90 Hz, 1H); 3.96 (s, 2H) ppm.
(amine protons are not visible due to H-D exchange)

**$^{13}$C-NMR** (101 MHz, 298 K DCM-$d_2$): $\delta$ = 145.52 (1C); 143.23 (2C); 143.21 (2C); 139.13 (2C); 137.78 (2C); 136.96 (2C); 136.77 (2C); 129.70 (4C); 128.46 (4C); 128.22 (4C); 128.05 (4C); 127.69 (4C); 121.43 (2C); 47.50 (1C) ppm.
(one carbon misses due to the signal to noise ratio)

**HRMS (ESI)** *m/z* calc. for $C_{37}H_{27}N + H^+$: 486.2216 $[M+H]^+$; found: 486.2219.

## ***N*-(Mesityl)-*N'*-(1-methylene-*meta*[6]cycloparaphenylene)oxalamide 3**

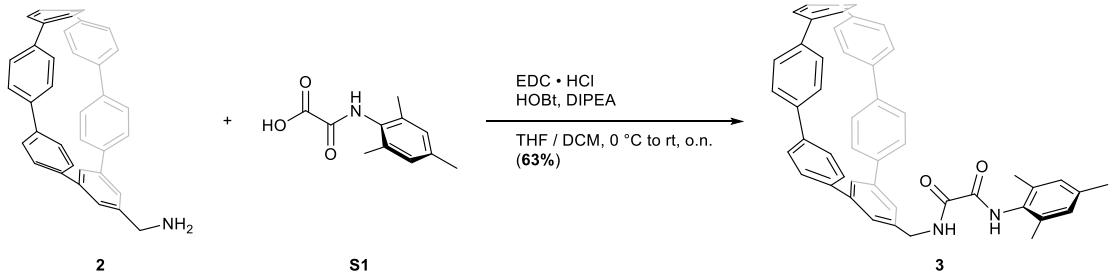


**2** **S1** **3**

*N*-(Mesityl)-oxanilic acid **S1** (59.7 mg, 288 µmol, 1.00 equiv.) and $^{i}Pr_2NEt$ (DIPEA, 123 µL, 720 mmol, 2.50 equiv.) were dissolved in THF (6 mL) and cooled to 0 °C. After addition of 1-hydroxybenzotriazole (60.2 mg, 432 µmol, 1.50 equiv.) and 1-ethyl-3-[3-dimethylaminopropyl]carbodiimide hydrochloride (66.3 mg, 346 µmol, 1.00 M in $CH_2Cl_2$, 1.20 equiv.) the reaction was stirred at this temperature until TLC showed full conversion (~1 h) of the oxanilic acid. At this point, amino-methylene-*meta*[6]cycloparaphenylene **2** (140 mg, 288 µmol, 1.00 equiv., in 2 mL THF) was added to the suspension and was allowed to stir overnight at rt. The next day, the reaction mixture was quenched with sodium bicarbonate, extracted with $CH_2Cl_2$ (3 x 50 mL), washed with water (3x50 mL), and brine (100 mL). The organic phase was dried over magnesium sulphate, and the volatiles were removed under reduced pressure, leaving a yellow solid, which was further purified by column chromatography ($SiO_2$, Cy/DCM/EtOAc = 5:1:1). The product **3** was obtained as a bright yellow solid (103 mg, 152 µmol, 53%).

**Mp.**: slow decomposition >230 °C.

**$^{1}$H-NMR** (400 MHz, 299 K; DCM-$d_2$): $\delta$ = 8.77 (s, 1H); 7.94 (s, 1H); 7.47 – 7.39 (m, 18H); 7.17 (m, 4H); 6.94 (s, 2H); 5.72 (t, $J$ = 1.76 Hz, 1H); 4.65 (d, $J$ = 6.36 Hz, 2H); 2.29 (s, 3H), 2.20 (s, 6H) ppm.

**$^{13}$C-NMR** (101 MHz, 300 K; DCM-$d_2$): $\delta$ = 160.23 (1C), 158.64 (1C), 143.56 (2C), 142.73 (2C), 139.33 (2C), 139.08 (1C), 138.77 (1C), 138.01 (1C), 137.84 (2C), 136.97 (2C), 136.73 (2C), 135.30 (2C), 130.41 (1C), 129.75 (4C), 129.31 (2C), 128.46 (4C), 128.24 (4C), 128.09 (4C), 127.73 (4C), 122.28 (2C), 44.42 (1C), 21.05 (1C), 18.50 (2C) ppm.

**IR (ATR)**: $\tilde{\nu}$ = 3304 (m), 3014 (m), 2919 (m), 2852 (m), 1659 (v), 1582 (m), 1496 (v) $cm^{-1}$.

**HRMS (ESI)** *m/z* calc. for $C_{48}H_{38}N_2O_2 + Na^+$: 697.2825 $[M+Na]^+$; found: 697.2817.

## Carboxy-*meta*[6]cycloparaphenylene 5

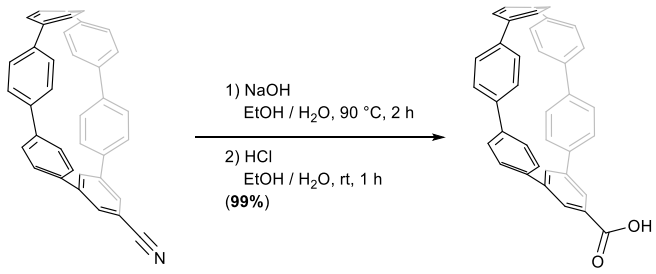


**1** **5**

This compound was synthesized according to literature[26] with slight modifications, preferable for the larger scale.
A suspension of cyano-*meta*[6]cycloparaphenylene **1** (300 mg, 623 µmol, 1.00 equiv.) in a solution of NaOH (5 N, 80 mL (EtOH/$H_2O$ = 1:1)) was stirred for 3 h at 90 °C. After cooling to rt, the solution was acidified to pH~2 and further stirred at rt for 1 h. The precipitate was filtered and washed with cold EtOH and water to remove excess of acid and inorganic salts. After drying under reduced pressure, the product **5** was obtained as a bright yellow solid (310 mg, 619 µmol, 99%).

**Mp.** = >280 °C (slow decomposition).

**$^1$H-NMR** (400 MHz, 297 K, DMSO-$d_6$): $\delta$ = 13.23 (s, 1H)*; 8.05 (d, $J$ = 1.85 Hz, 2H); 7.60 – 7.52 (m, 16H), 7.24 – 7.21 (m, 4H); 5.67 (t, $J$ = 1.85 Hz, 1H) ppm.
(*proton of carboxylic acid exchanges with water from solvent.)

**$^{13}$C-NMR** (101 MHz, 297 K DMSO-$d_6$): $\delta$ = 167.19 (1C); 142.33 (2C); 142.22 (1C); 141.03 (2C); 138.55 (2C); 136.80 (2C); 135.62 (2C); 134.96 (2C); 132.52 (1C); 129.33 (4C); 128.02 (4C); 127.78 (4C); 127.72 (4C); 127.40 (4C); 122.96 (2C) ppm.

**IR (ATR)**: $\tilde{\nu}$ = 2853 (m); 1898 (w); 1716 (m); 1681 (s); 1578 (s); 1483 (m) cm$^{-1}$.

**HRMS (ESI)** *m/z* calc. for $C_{37}H_{24}O_2$ + $H^+$: 501.1849 [*M*+H]$^+$; found 501.1842.

## Bromo-methylene-*meta*[6]cycloparaphenylene 6

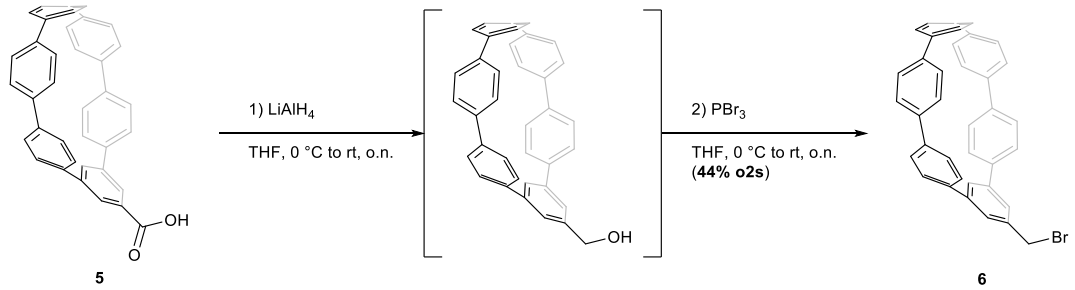


A solution of carboxy-*meta*[6]cycloparaphenylene **6** (250 mg, 500 µmol, 1.00 equiv.) in THF (20 mL) was cooled to -20 °C. After careful addition of $LiAlH_4$ (40.0 mg, 1.00 µmol, 2.00 equiv.) the reaction mixture was allowed to warm up to rt and stirred overnight. The reaction was quenched at 0 °C using a saturated sodium/potassium tartrate solution (200 mL). After warming up to rt, diethyl ether (100 mL) was added, and the organic layer was separated. After extraction with diethyl ether (3x100 mL), the combined organic layers were washed with saturated sodium biscarbonate solution (3x100 mL). After drying over magnesium sulphate, and subsequent filtration, the volatiles have been removed at the rotary evaporator to afford the crude benzylic alcohol, which was used without further purification.

After cooling a solution of the afforded crude alcohol in THF (10 mL) to 0 °C, $PBr_3$ (68 µL, 0.25 mmol, 0.50 equiv.) was added dropwise to the reaction. The reaction was warmed up to rt and stirred overnight. After dropwise addition of water (5 mL), diethyl ether (50 mL) was added, and the organic phase has been separated. After extraction with diethyl ether (3 x 50 mL), the combined organic layers were washed with saturated sodium bis carbonate solution (3 x 50 mL). After drying over magnesium sulphate, and subsequent filtration, the volatiles have been removed at the rotary evaporator to afford the crude benzylic bromine. Further purification using flash column chromatography ($SiO_2$, Cy/DCM = 6:1) afforded the desired product **6** (120 mg, 218 µmol, 44%).

**Mp.** = >290 °C (slow decomposition).

**$^1$H-NMR** (400 MHz, 297 K, DCM-$d_2$): $\delta$ = 7.49 (d, $J$ = 1.68 Hz, 2H)*; 7.45 – 7.39 (m, 16H)*; 7.16 – 7.13 (m, 4H)*; 5.72 (t, $J$ = 1.68 Hz, 1H); 4.64 (s, 2H) ppm.

*Partial hydrolysis under ambient conditions while attempting to remove solvent residues (DCM worked well, but diethyl ether still inside). Water (1.53 ppm) from NMR solvent.

**$^{13}$C-NMR** (101 MHz, $CD_2Cl_2$): $\delta$ = 143.52 (2C); 142.42 (2C); 139.76 (2C); 139.45 (1C); 139.36 (1C); 137.83 (2C); 136.95 (2C); 136.70 (2C); 129.75 (4C); 128.45 (4C); 128.24 (4C); 128.10 (4C); 127.75 (4C); 123.35 ($2C_q$); 34.35 (1C) ppm.

*$\delta$ = 66.07 (2C); 15.51 (2C) ppm correspond to diethyl ether which could not be removed.

**IR (ATR)**: $\tilde{\nu}$ = 2850 (m); 1892 (w); 1638 (m); 1580 (s) 1482 (m) $cm^{-1}$.

**HRMS (APCI)** *m/z* calc. for $C_{37}H_{25}Br + H^+$: 549.1213 $[M+H]^+$; found 549.1213.

## ***N*-(Methyl)-*N'*-(1-methylene-*meta*[6]cycloparaphenylene)-imidazolium bromide 7**

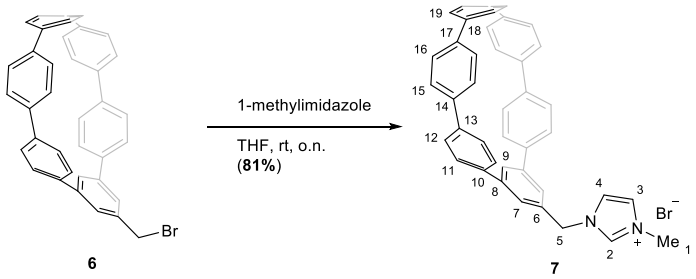


To a solution of bromo-methylene-*meta*[6]cycloparaphenylene **6** (100 mg, 182 µmol, 1.00 equiv.) in THF (10 mL) *N*-methyl-imidazole (0.10 mL, 1.2 mmol, 6.6 equiv.) was added at rt and was stirred overnight. The next day, the precipitate was filtered over a plug of Celite® and washed with cold diethyl ether until the filtrate became colourless. Then, the solvent has been changed to MeCN, and the desired product **9** was eluted. After removing the volatiles at the rotary evaporator, the desired product **7** was obtained as a yellow solid (93.0 mg, 147 µmol, 81%).

**Mp.** = >290 °C (slow decomposition)

**$^1$H-NMR** (400 MHz, 297 K, MeCN-$d_3$): $\delta$ = 8.91 (s, $1H_2$); 7.57 – 7.56 (m, $2H_7$); 7.56 – 7.46 (m, $17H_{4,\ 12,15,16,19}$); 7.40 (t, $J$ = 1.86 Hz, $1H_3$)[(a)]; 7.24 – 7.18 (m, $4H_{11}$); 5.54 (t, $J$ = 1.76 Hz, $1H_9$); 5.48 (s, $2H_5$); 3.87 (s, $3H_1$) ppm.

[(a)]Coupling partner underneath the multiplet 7.57 – 7.50 ppm.

*Water (2.16 ppm) from NMR solvent.

**$^{13}$C-NMR** (101 MHz, 298 K, DCM-$d_2$): $\delta$ = 144.46 (2C); 142.84 (2C); 140.35 ($1C_9$); 140.19 (2C); 138.71 (2C); 137.62 (2C); 137.50 ($1C_2$); 137.11 (2C); 136.72 ($1C_6$); 130.29 ($4C_{11}$); 129.26 (4C); 129.10 (4C); 128.81 (4C); 128.45 (4C); 125.08 ($1C_3$); 123.47 ($2C_7$); 123.36 ($1C_4$); 53.73 ($1C_5$); 37.05 ($1C_1$) ppm.

**IR (ATR)**: $\tilde{\nu}$ = 3012 (m); 1890 (w); 1570 (s); 1481 (m) $cm^{-1}$.

**HRMS (ESI)** *m/z* calc. for $C_{41}H_{31}BrN_2$ - $Br^-$ 551.2482 $[M\text{-}Br^-]^+$; found 551.2498.

## [*N*-(Methyl)-*N'*-(1-methylene-*meta*[6]cycloparaphenylene)-imidazolium]gold bromide 8

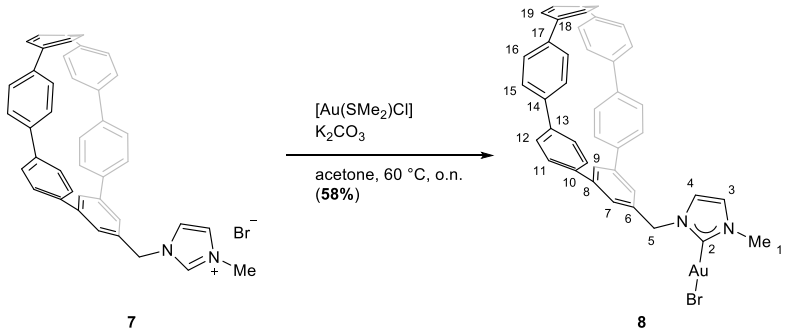


**7** **8**

To a solution of imidazolium bromide **7** (20.0 mg, 31.7 µmol, 1.00 equiv.) in acetone (2 mL) was added grinded $K_2CO_3$ (13.1 mg, 95.1 µmol, 3.0 equiv.) and [Au($SMe_2$)Cl] (9.63 mg, 31.7 µmol, 1.0 equiv.). The solution was stirred at 60 °C overnight. After cooling to rt, the solvent was evaporated, and the resulting solid was suspended in diethyl ether before filtered over a Celite® plug. After washing with excess cold diethyl ether, the yellow solid was eluted using DCM. After evaporation of the volatiles, the product was further purified by flash column chromatography ($SiO_2$, Cy/DCM = 1:3) to obtain complex **8** as a yellow solid (15.2 mg, 18.3 µmol, 58%).

**Mp.** = >290 °C (slow decomposition)

**$^1$H-NMR** (400 MHz, 297 K, $CDCl_3$): $\delta$ = 7.44 – 7.38 (m, 16$H_{12,15,16,19}$); 7.34 (d, $J$ = 1.76 Hz, 2$H_7$); 7.14 – 7.11 (m, 4$H_{11}$); 6.95 (d, $J$ = 7.77 Hz, 1$H_4$)[(a)]; 6.95 (d, $J$ = 7.77 Hz, 1$H_3$)[(a)]; 5.58 (t, $J$ = 1.76 Hz, 1$H_9$); 5.48 (s, 2$H_5$); 3.88 (s, 3$H_1$) ppm.

(a) Overlapping doublets caused by the imidazolium backbone.

**$^{13}$C-NMR** (101 MHz, 297 K, $CDCl_3$): $\delta$ = 175.55 (1$C_2$); 143.66 (2C); 141.74 (2C); 140.06 (1$C_9$); 139.57 (2C); 137.68 (2C); 136.55 (2C); 136.32 (2C); 136.29 (1C); 129.57 (4C); 128.22 (4C); 128.00 (4C); 127.74 (4C); 127.41 (4C); 122.41 (1$C_3$); 121.86 (2$C_7$); 120.52 (1$C_4$); 55.31 (1$C_1$); 38.41 (1$C_1$) ppm.

**IR (ATR)**: $\tilde{\nu}$ = 3013 (m); 1885 (w); 1568 (s); 1482 (m) cm$^{-1}$.

**HRMS (APCI)** *m/z* calc. for $C_{41}H_{30}AuBrN_2$ 827.1336 [*M*+H]$^+$; found 827.1334.

**EA** Found: C, 55.3; H, 3.6. Calc. for $C_{41}H_{30}N_2AuBr \bullet CH_2Cl_2$: C, 55.3; H, 3.5% ($CH_2Cl_2$ has been used for column chromatography. It has been observed before that a $CH_2Cl_2$ was included in the solid-state structure in the middle of a CPP)

# 3. Photophysical Characteristics

**UV-vis- and emission spectra**: All UV-vis-measurements were performed in HPLC-grade chloroform under ambient conditions in concentrations ranging from $3.3 \cdot 10^{-6}$ M to $5.0 \cdot 10^{-7}$ M. The samples for emission spectra were excited at the corresponding absorption maximum and measured in a range from 350 nm to 750 nm.

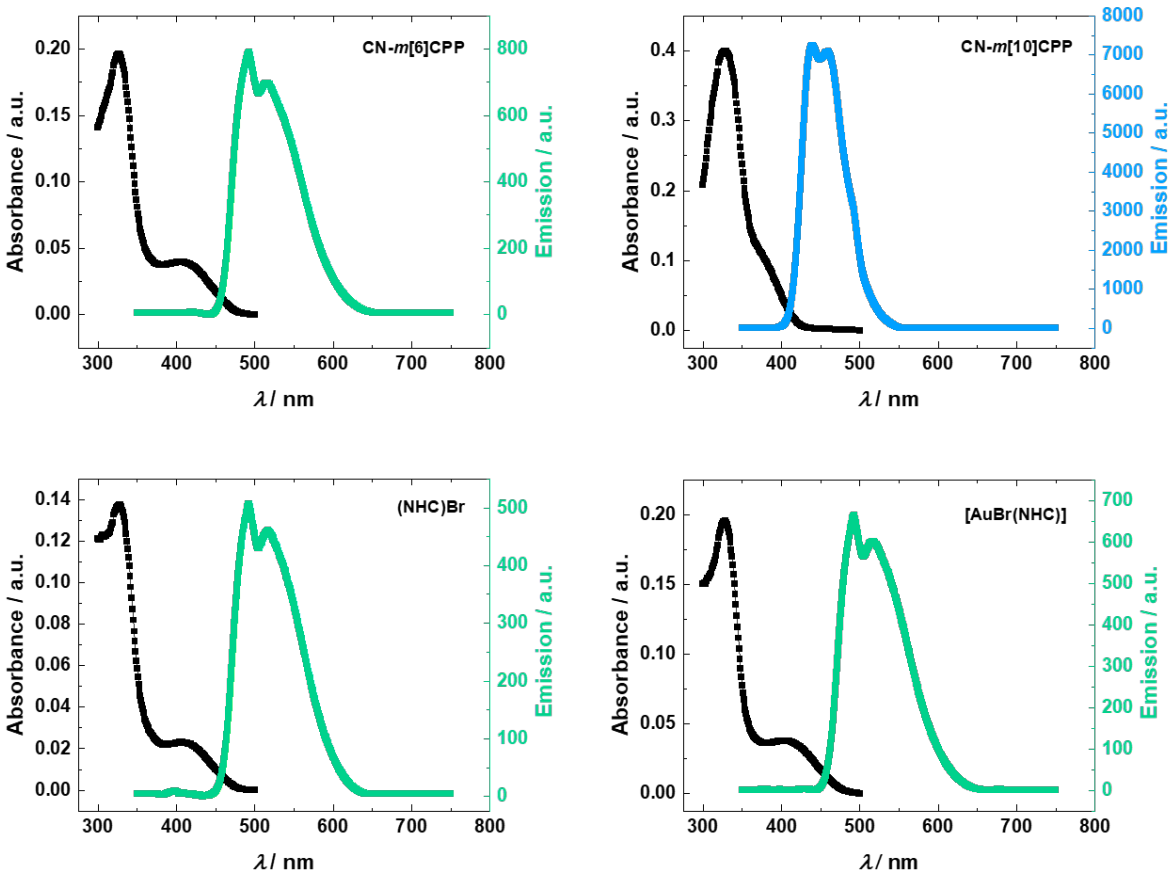


**Figure S1.** Absorbance (left) and emission (right) spectra of the investigated compounds. The literature-known compounds cyano-*meta*[6]cycloparaphenylene (top, left) and cyano-*meta*[10]cycloparaphenylene (top, right) have been remeasured in regards to the determination of the fluorescence quantum yield. Imidazolium bromide **7** (bottom, left) and [AuBr(NHC)] complex **8** (bottom, right).

**Determination of the molar extinction coefficients and relative fluorescence quantum yields:** The fluorescence quantum yields of the imidazolium bromide **7** and the [AuBr(NHC)] complex **8** were measured according to a literature procedure.[27] All measurements were carried out in HPLC-grade chloroform while using a constant slid width (2.5 nm) with an excitation wavelength of 326 nm, and an integration from 350 nm – 750 nm for all compounds measured. For calibration of these measurements CN-*m*[6]CPP ($\phi_{\text{CN-}m\text{[6]CPP}}$ = 0.24[26]) and CN-*m*[10]CPP ($\phi_{\text{CN-}m\text{[10]CPP}}$ = 0.71[26]) in chloroform were chosen as internal standards. Therefore, a cross-calibration using the two CPP standards has been performed. After measuring a serial dilution of both the absorbance and the emission, the integrated emission intensity is plotted against the absorbance.

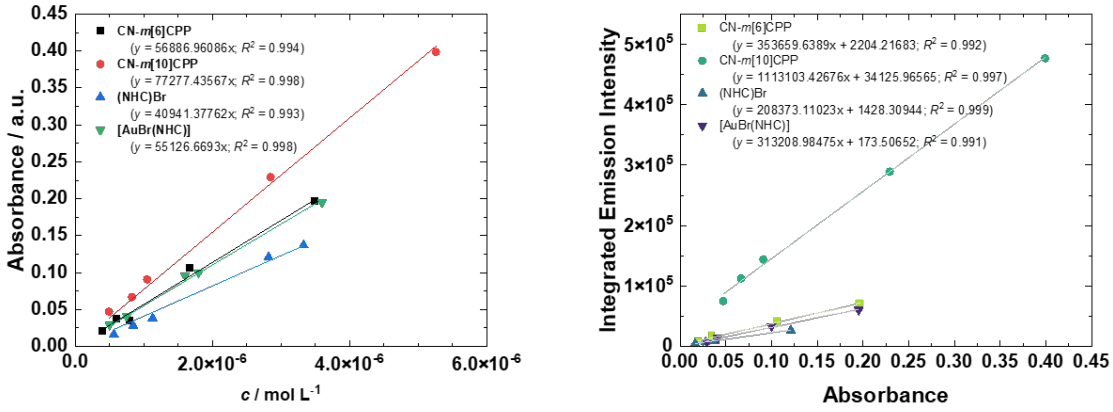


**Figure S2.** Determination of the extinction coefficient at $\lambda_{abs,max}$ (left) and the relative fluorescence quantum yield (right).

After measuring a serial dilution of both the absorbance and the emission, the integrated emission intensity is plotted against the absorbance. The obtained slope was then used in Equation S1 to calculate the relative fluorescence quantum yield of the desired compound. The error of the cross-calibration must be within 10% of the published data for reliable results.

$$\phi_{\text{CN}-m\text{[6]CPP}} / \phi_{\text{CN}-m\text{[10]CPP}} = m_{\text{CN}-m\text{[6]CPP}} / m_{\text{CN}-m\text{[10]CPP}} \cdot \eta_{CHCl_3} / \eta_{CHCl_3} \qquad \textbf{(S1)}$$

$$\phi_{\text{CN}-m\text{[6]CPP}} = \phi_{\text{CN}-m\text{[10]CPP}} \cdot m_{\text{CN}-m\text{[6]CPP}} / m_{\text{CN}-m\text{[10]CPP}} = 0.71 \cdot 353660 / 1113103 = 0.23$$

$$\Delta_{\text{rel}} = |0.24 - 0.23| / 0.24 = 0.04$$

The methodology is suitable for our calibration system as the relative error is below 0.10.

**Excitation spectra:** All excitation measurements were performed in HPLC-grade chloroform under ambient conditions in concentrations of $3.3 \cdot 10^{-6}$ M. The samples for excitation spectra were excited at the corresponding emission maxima and measured in a range from 300 nm to 490 nm.

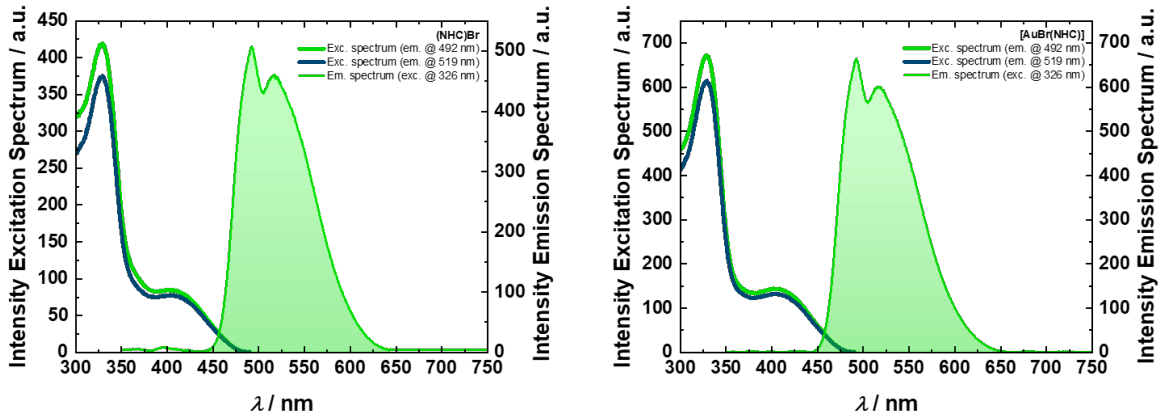


**Figure S3.** Excitation (curves with white area) and emission (curves with green area) spectra of the imidazolium bromide (**7**, left) and the [AuBr(NHC)]-complex (**8**, right).

The spectroscopic characteristics determined within our studies are summarised in Table S1.

**Table S1.** Summarised spectroscopic characteristics, collected within this study.

| | $\lambda_{abs,max}$ / nm | $\varepsilon_{\lambda abs,max}$ / (M cm)$^{-1}$ | $\lambda_{em,max}$ / nm | $\lambda_{em,max}$ / nm | $\Phi_{max}$ | $\lambda_{exc,max}$ / nm |
|---|---|---|---|---|---|---|
| CN-*m*[6]CPP[26] | 327 | $5.7 \cdot 10^4$ | 493 | 519 | 0.24 | - |
| CN-*m*[10]CPP[26] | 328 | $7.3 \cdot 10^4$ | 440 | 458 | 0.71 | - |
| **(NHC)Br** | 327 | $4.1 \cdot 10^4$ | 492 | 516 | 0.14 | 328 |
| **[AuBr(NHC)]** | 327 | $5.5 \cdot 10^4$ | 492 | 516 | 0.21 | 328 |

# 4. Structural Data

**Solid-state structure of *N*-(methyl)-*N'*-(1-methylene-*meta*[6]cycloparaphenylene)-imidazolium bromide 7 [CCDC No. 2303780]**

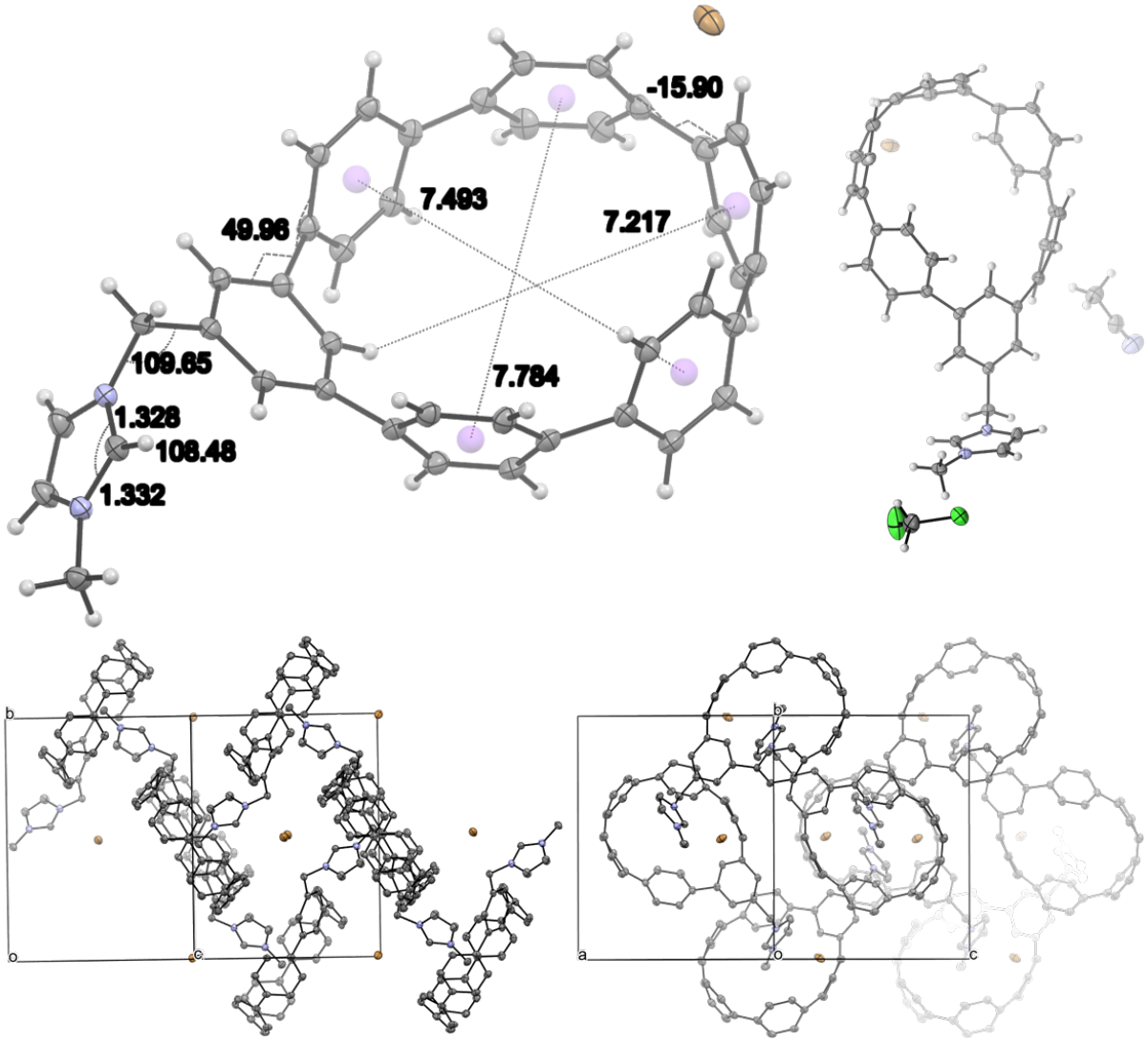


**Figure S4.** ORTEP drawing of the solid-state structure of *N*-(methyl)-*N'*-(1-methylene-*meta*[6]cycloparaphenylene)-imidazolium bromide **7** with the most important structural parameters shown (top, left). ORTEP drawing of **7**'s solid-state structure with defined acetonitrile and dichloromethane molecules (top right). Crystal packing structures of compound **7** in the solid-state structure at different orientations (bottom). Solvent molecules and protons have been omitted for clarity.

**Table S2.** Crystal data and structure refinement for *N*-(methyl)-*N*'-(1-methylene-*meta*[6]cycloparaphenylene)-imidazolium bromide **7**. Additional data can be found on the Cambridge Structural Database and the FIZ Karlsruhe, using the CCDC No. 2303780.

| **CCDC No.** | **2303780** | |
|---|---|---|
| **Empirical formula** | $C_{44}H_{36}BrCl_2N_3$ | |
| **Formula weight** | 757.57 | |
| **Temperature** | 100(2) K | |
| **Wavelength** | 0.71073 Å | |
| **Crystal system** | Monoclinic | |
| **Space group** | $P2_1/c$ | |
| **Unit cell dimensions** | $a$ = 15.5477(17) Å | $\alpha$ = 90°. |
| | $b$ = 14.2729(13) Å | $\beta$ = 92.941(4)°. |
| | $c$ = 16.1793(16) Å | $\gamma$ = 90°. |
| **Volume** | 3585.6(6) $Å^3$ | |
| **Z** | 4 | |
| **Density (calculated)** | 1.403 $Mg/m^3$ | |
| **Absorption coefficient** | 1.332 $mm^{-1}$ | |
| **F(000)** | 1560 | |
| **Crystal size** | 0.352 x 0.257 x 0.215 $mm^3$ | |
| **Theta range for data collection** | 1.938 to 31.505°. | |
| **Index ranges** | -22<=h<=22, -20<=k<=20, -23<=l<=23 | |
| **Reflections collected** | 457779 | |
| **Independent reflections** | 11920 [R(int) = 0.1070] | |
| **Completeness to theta = 25.242°** | 100.0 % | |
| **Absorption correction** | None | |
| **Max. and min. transmission** | 0.7448 and 0.6765 | |
| **Refinement method** | Full-matrix least-squares on $F^2$ | |
| **Data / restraints / parameters** | 11920 / 0 / 454 | |
| **Goodness-of-fit on $F^2$** | 1.023 | |
| **Final R indices [I>2sigma(I)]** | R1 = 0.0666, wR2 = 0.1907 | |
| **R indices (all data)** | R1 = 0.0854, wR2 = 0.2144 | |
| **Extinction coefficient** | n/a | |
| **Largest diff. peak and hole** | 2.213 and -2.198 $e.Å^{-3}$ | |

**Solid-state structure [*N*-(Methyl)-*N'*-(1-methylene-*meta*[6]cycloparaphenylene)-imidazolium]gold bromide 8 [CCDC No. 2310446]**

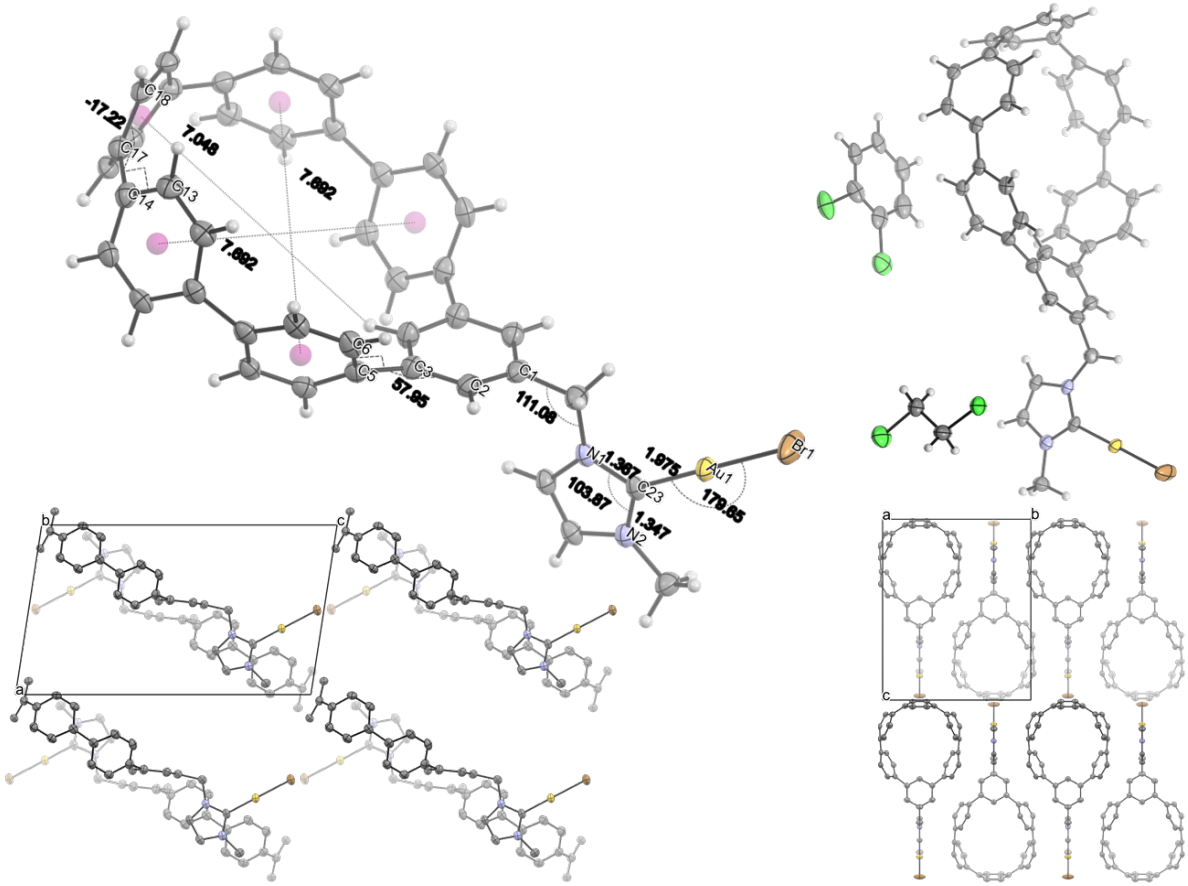


**Figure S5.** ORTEP drawing of the solid-state structure of [*N*-(Methyl)-*N'*-(1-methylene-*meta*[6]cycloparaphenylene)-imidazolium]gold bromide **8** with the most important structural parameters shown (top, left). ORTEP drawing of **8**'s solid-state structure with both one defined 1,2-dichloro ethane and one defined 1,2-dichloro benzene molecule (top, right). Crystal packing structures of compound **10** in the solid-state structure at different orientations (bottom). Solvent molecules and protons have been omitted for clarity.

**Table S3.** Crystal data and structure refinement for [*N*-(methyl)-*N*'-(1-methylene-*meta*[6]cycloparaphenylene)-imidazolium]gold bromide **8**. Additional data can be found on the Cambridge Structural Database and the FIZ Karlsruhe, using the CCDC No. 2310446.

| **CCDC No.** | **2310446** | |
|---|---|---|
| **Empirical formula** | $C_{57}H_{46}AuBrCl_8N_2$ | |
| **Formula weight** | 1319.43 | |
| **Temperature** | 100(2) K | |
| **Wavelength** | 0.71073 Å | |
| **Crystal system** | Monoclinic | |
| **Space group** | $P2_1/m$ | |
| **Unit cell dimensions** | a = 10.2999(5) Å | α = 90°. |
| | b = 14.4369(8) Å | *β* = 98.815(2)°. |
| | c = 17.7726(9) Å | *γ* = 90°. |
| **Volume** | 2611.5(2) $Å^3$ | |
| **Z** | 2 | |
| **Density (calculated)** | 1.678 $Mg/m^3$ | |
| **Absorption coefficient** | 4.032 $mm^{-1}$ | |
| **F(000)** | 1304 | |
| **Crystal size** | 0.255 x 0.142 x 0.059 $mm^3$ | |
| **Theta range for data collection** | 2.153 to 25.349°. | |
| **Index ranges** | -12<=h<=12, -17<=k<=17, -21<=l<=21 | |
| **Reflections collected** | 125126 | |
| **Independent reflections** | 4990 [R(int) = 0.0590] | |
| **Completeness to theta = 25.242°** | 99.9 % | |
| **Absorption correction** | Semi-empirical from equivalents | |
| **Max. and min. transmission** | 0.7465 and 0.5504 | |
| **Refinement method** | Full-matrix least-squares on $F^2$ | |
| **Data / restraints / parameters** | 4990 / 91 / 401 | |
| **Goodness-of-fit on $F^2$** | 1.095 | |
| **Final R indices [I>2sigma(I)]** | R1 = 0.0471, wR2 = 0.1150 | |
| **R indices (all data)** | R1 = 0.0487, wR2 = 0.1163 | |
| **Extinction coefficient** | n/a | |
| **Largest diff. peak and hole** | 2.497 and -2.128 e.$Å^{-3}$ | |

## Generation and results of the steric map using the online-tool SambVCA 2.1:

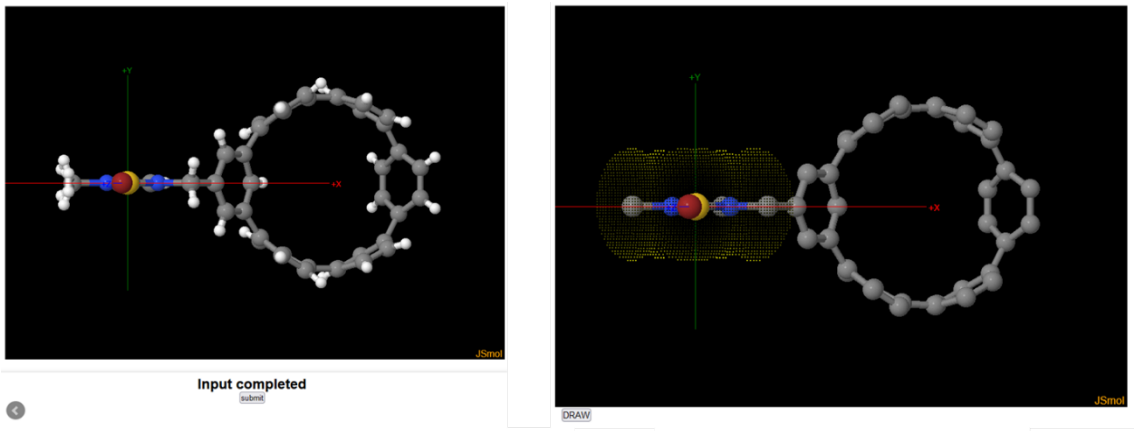


| %V Free | %V Buried | % V Tot/V Ex |
|---|---|---|
| 73.5 | 26.5 | 99.9 |

| Quadrant | V f | V b | V t | %V f | %V b |
|---|---|---|---|---|---|
| SW | 33.1 | 11.8 | 44.9 | 73.8 | 26.2 |
| NW | 33.1 | 11.8 | 44.9 | 73.8 | 26.2 |
| NE | 32.8 | 12.0 | 44.9 | 73.2 | 26.8 |
| SE | 32.8 | 12.0 | 44.9 | 73.2 | 26.8 |

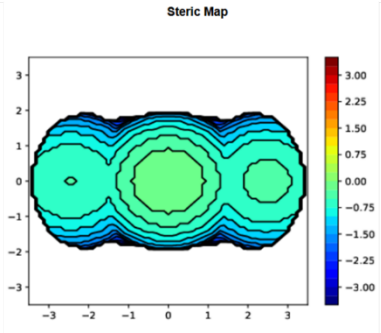


**Figure S6.** Original data from the online-tool SambVCA 2.1 for the solid-state structure of [AuBr(NHC)] complex **8**.

# 5. Theoretical Calculation

## Geometry data and Gibbs energy

**Table S4.** Geometries and Gibbs energy of [AuBr(NHC)] complex **8**.

| 75 | AuC41N2H30Br | G = -23989.1402742 Eh | |
|---|---|---|---|
| **Element** | **X** | **Y** | **Z** |
| **N** | -5.011239000 | 0.613974000 | 1.081409000 |
| **N** | -5.439882000 | 1.528907000 | -0.801854000 |
| **C** | -2.944670000 | -0.142475000 | 2.183633000 |
| **C** | -2.339495000 | 1.111037000 | 2.142048000 |
| **H** | -2.944119000 | 2.000413000 | 1.998237000 |
| **C** | -0.956627000 | 1.220345000 | 2.230337000 |
| **C** | -0.210923000 | 0.053826000 | 2.388977000 |
| **H** | 0.869146000 | 0.126999000 | 2.375550000 |
| **C** | -0.789664000 | -1.211748000 | 2.369175000 |
| **C** | -2.175884000 | -1.298337000 | 2.270136000 |
| **H** | -2.659554000 | -2.268153000 | 2.219194000 |
| **C** | -0.160907000 | 2.429578000 | 1.927725000 |
| **C** | 0.999150000 | 2.699682000 | 2.654129000 |
| **H** | 1.144777000 | 2.232616000 | 3.622054000 |
| **C** | 2.032048000 | 3.425003000 | 2.092599000 |
| **H** | 2.972161000 | 3.489146000 | 2.627298000 |
| **C** | 1.948246000 | 3.899447000 | 0.779018000 |
| **C** | 0.695908000 | 3.837695000 | 0.158950000 |
| **H** | 0.561859000 | 4.254269000 | -0.833074000 |
| **C** | -0.341648000 | 3.111443000 | 0.723060000 |
| **H** | -1.252584000 | 2.958981000 | 0.153645000 |
| **C** | 3.208131000 | 4.038767000 | 0.020130000 |
| **C** | 3.247680000 | 3.529906000 | -1.280698000 |
| **H** | 2.325884000 | 3.382084000 | -1.830442000 |
| **C** | 4.408647000 | 2.982863000 | -1.793062000 |
| **H** | 4.343881000 | 2.425872000 | -2.719769000 |
| **C** | 5.575651000 | 2.922235000 | -1.024619000 |
| **C** | 5.605666000 | 3.718226000 | 0.128505000 |
| **H** | 6.520011000 | 3.805663000 | 0.704750000 |
| **C** | 4.442571000 | 4.261519000 | 0.643443000 |
| **H** | 4.481540000 | 4.760350000 | 1.605614000 |
| **C** | 6.438595000 | 1.734403000 | -1.188184000 |
| **C** | 6.905562000 | 1.112054000 | -0.026044000 |
| **H** | 6.999298000 | 1.680991000 | 0.890990000 |
| **C** | 6.999136000 | -0.264242000 | 0.051190000 |
| **H** | 7.162306000 | -0.710026000 | 1.024864000 |
| **C** | 6.628353000 | -1.069394000 | -1.030549000 |
| **C** | 6.515236000 | -0.428229000 | -2.272094000 |
| **H** | 6.355827000 | -1.010826000 | -3.172678000 |
| **C** | 6.421742000 | 0.949390000 | -2.349459000 |
| **H** | 6.192250000 | 1.401025000 | -3.308263000 |
| **C** | 5.934559000 | -2.338469000 | -0.729882000 |
| **C** | 6.065731000 | -2.991482000 | 0.503137000 |
| **H** | 6.979259000 | -2.888631000 | 1.078200000 |
| **C** | 4.985475000 | -3.631829000 | 1.083060000 |
| **H** | 5.086257000 | -4.013482000 | 2.093176000 |
| **C** | 3.736273000 | -3.650319000 | 0.449633000 |
| **C** | 3.713614000 | -3.284409000 | -0.898872000 |
| **H** | 2.783968000 | -3.326082000 | -1.453680000 |
| **C** | 4.791504000 | -2.641201000 | -1.476888000 |
| **H** | 4.656988000 | -2.202728000 | -2.458175000 |
| **C** | 2.463707000 | -3.607838000 | 1.199041000 |
| **C** | 1.220274000 | -3.784424000 | 0.583794000 |

| | | | |
|---|---|---|---|
| **H** | 1.151581000 | -4.314668000 | -0.359460000 |
| **C** | 0.087635000 | -3.152657000 | 1.073489000 |
| **H** | -0.825650000 | -3.182737000 | 0.488684000 |
| **C** | 0.164528000 | -2.328400000 | 2.197068000 |
| **C** | 1.344141000 | -2.356846000 | 2.941772000 |
| **H** | 1.416176000 | -1.773079000 | 3.853052000 |
| **C** | 2.471402000 | -2.989482000 | 2.454446000 |
| **H** | 3.407141000 | -2.866935000 | 2.986725000 |
| **C** | -4.440970000 | -0.266231000 | 2.087992000 |
| **H** | -4.716209000 | -1.294044000 | 1.849151000 |
| **H** | -4.914605000 | -0.006892000 | 3.036970000 |
| **C** | -4.748773000 | 0.521455000 | -0.238228000 |
| **C** | -5.850251000 | 1.669243000 | 1.341250000 |
| **H** | -6.175572000 | 1.911652000 | 2.338789000 |
| **C** | -6.123036000 | 2.247456000 | 0.150673000 |
| **H** | -6.737191000 | 3.095555000 | -0.100299000 |
| **C** | -5.470547000 | 1.828508000 | -2.217382000 |
| **H** | -4.849580000 | 1.100428000 | -2.734513000 |
| **H** | -5.080371000 | 2.831287000 | -2.392328000 |
| **H** | -6.493846000 | 1.765111000 | -2.587738000 |
| **Au** | -3.565136000 | -0.810668000 | -1.119248000 |
| **Br** | -2.131657000 | -2.432257000 | -2.189844000 |

## Molecular Orbitals

**Table S5.** Molecular orbitals derived from TD-DFT calculations at a PBE0/ZORA-def2-TZVPP/D3BJ/CPCM(CHCl3) level of theory with a separate GTO for the gold atom (SARC-ZORA-TZVPP).

| Description | Graphical Representation | Energy / eV |
|---|---|---|
| **LUMO+5** | 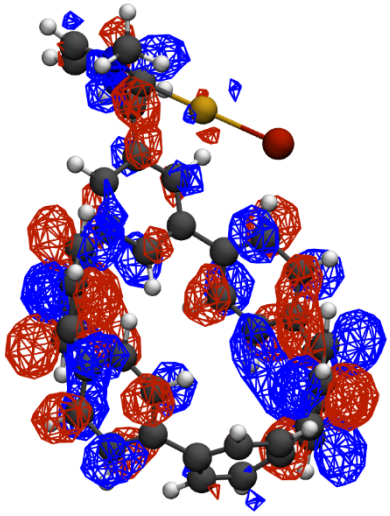 | -0.4870 |
| **LUMO+4** | 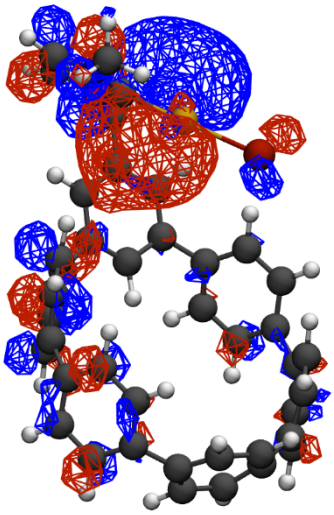 | -0.6284 |

| | | |
|---|---|---|
| **LUMO+3** | 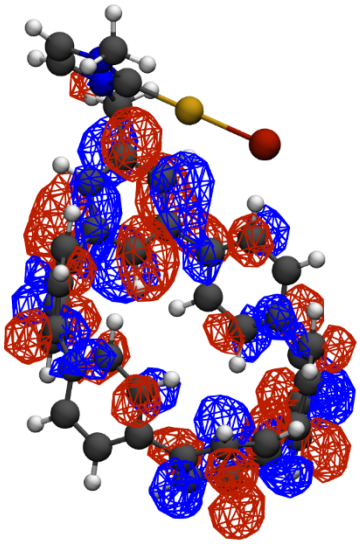 | -0.6950 |
| **LUMO+2** | 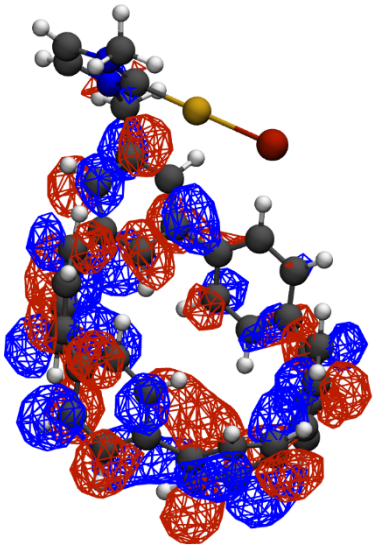 | -0.7222 |
| **LUMO+1** | 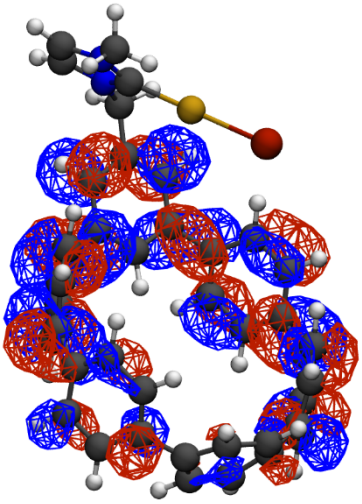 | -1.4407 |

| | | |
|---|---|---|
| **LUMO** | 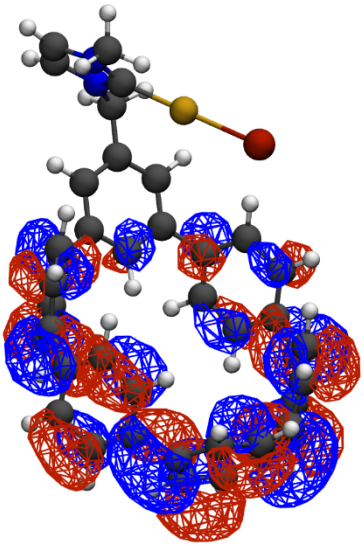 | -1.8592 |
| **HOMO** | 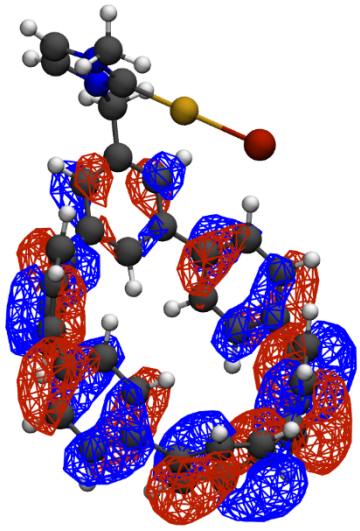 | -5.5549 |
| **HOMO-1** | 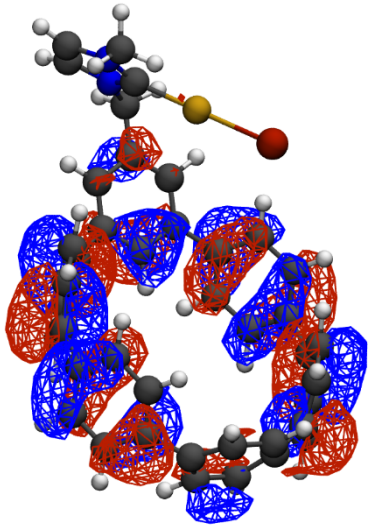 | -6.2120 |

| | | |
|---|---|---|
| **HOMO-2** | 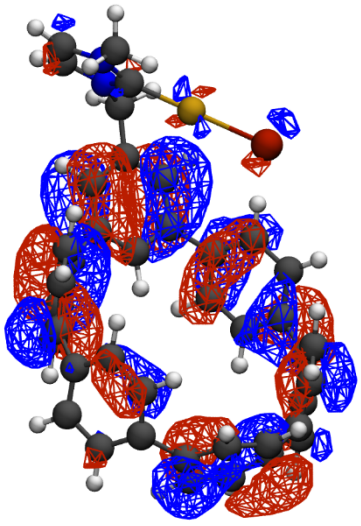 | -6.7161 |
| **HOMO-3** | 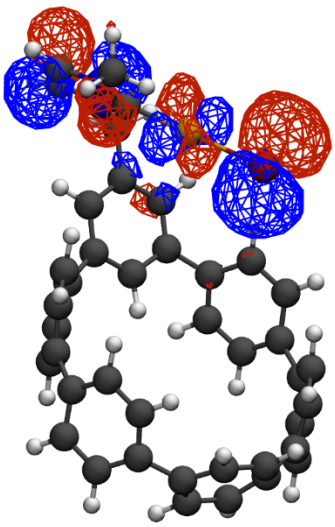 | -6.7913 |
| **HOMO-4** | 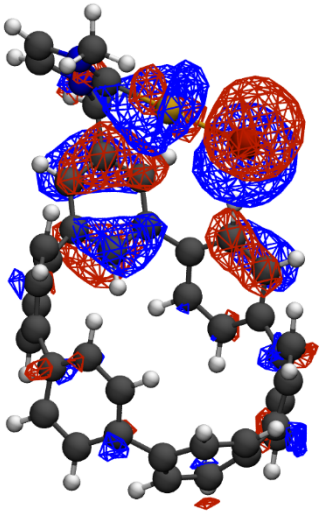 | -7.0194 |

| | | |
|---|---|---|
| **HOMO-5** | 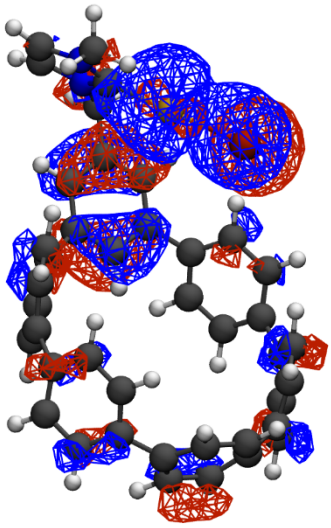 | -7.1611 |
| **HOMO-6** | 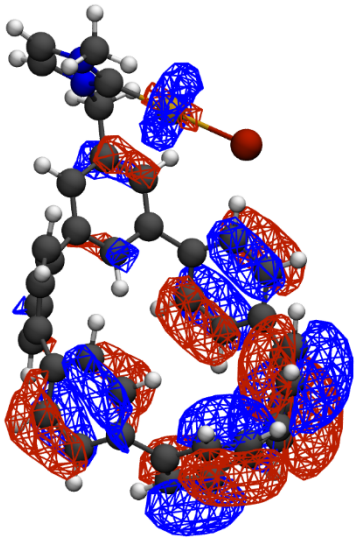 | -7.2380 |
| **HOMO-7** | 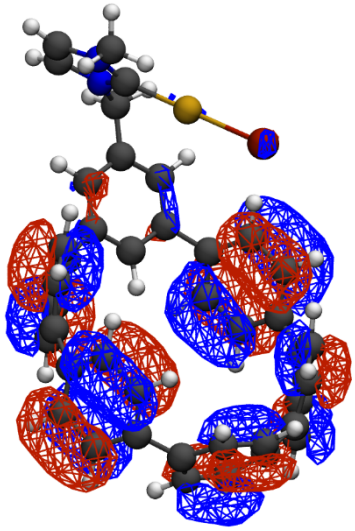 | -7.3086 |

| | | |
|---|---|---|
| **HOMO-8** | 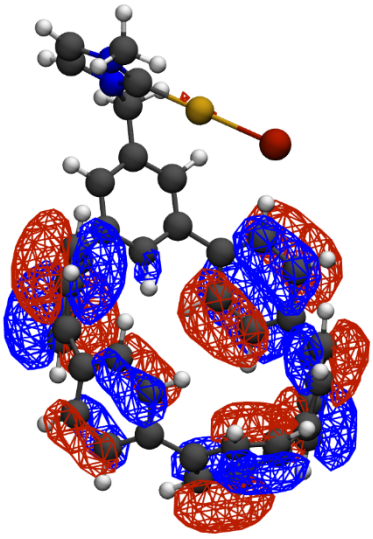 | -7.3982 |

**Table S6.** First six electronic states with weight of excitations if ≥2.0·10$^{-2}$.

| #State | Excitation | | |
|---|---|---|---|
| | From | To | Weight |
| **State 1: (412.1 nm)** | HOMO | LUMO | 0.96 |
| | HOMO-1 | LUMO+1 | 0.02 |
| **State 2: (346.9 nm)** | HOMO | LUMO+1 | 0.86 |
| | HOMO-1 | LUMO | 0.12 |
| **State 3: (322.1 nm)** | HOMO-1 | LUMO | 0.84 |
| | HOMO | LUMO+1 | 0.11 |
| **State 4: (310.5 nm)** | HOMO | LUMO+2 | 0.54 |
| | HOMO | LUMO+3 | 0.22 |
| | HOMO-6 | LUMO | 0.09 |
| **State 5: (304.2 nm)** | HOMO-1 | LUMO+1 | 0.82 |
| | HOMO-3 | LUMO+1 | 0.05 |
| | HOMO | LUMO+3 | 0.05 |
| **State 6: (295.0 nm)** | HOMO | LUMO+5 | 0.35 |
| | HOMO | LUMO+3 | 0.16 |
| | HOMO | LUMO+4 | 0.13 |
| | HOMO | LUMO+2 | 0.08 |
| | HOMO-7 | LUMO | 0.06 |
| | HOMO-1 | LUMO+2 | 0.03 |
| | HOMO-2 | LUMO | 0.03 |
| | HOMO-8 | LUMO | 0.02 |

## Absorption Spectrum via Transition Electric Dipole Moments

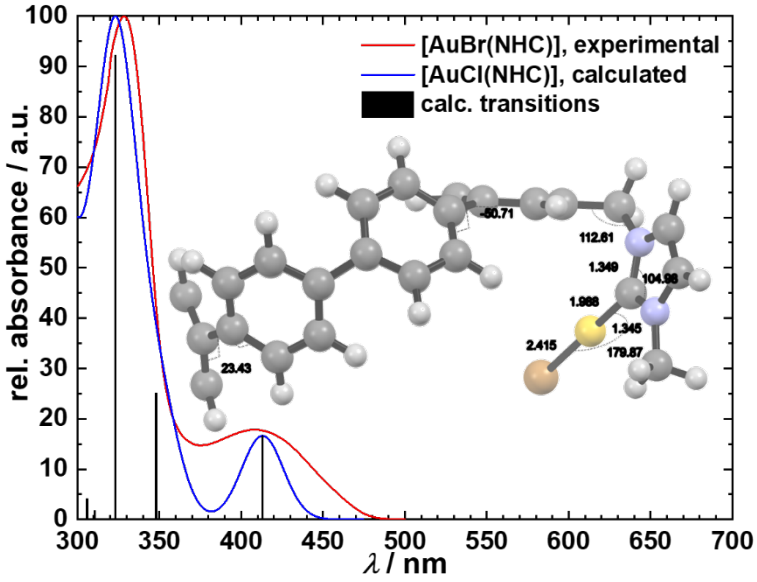


**Figure S7.** Comparison of the experimental (red) and theoretically calculated (blue) UV/Vis-spectrum of [AuBr(NHC)] complex **8**. Additionally, the ground-state geometry of complex **8** is shown.

**Table S7.** Electronic states and their corresponding energies, wavelengths, and oscillator strengths.

| State | $E$ (cm$^{-1}$) | $\lambda$ (nm) | $F_{osc}$ |
|---|---|---|---|
| **1** | 24266.6 | 412.1 | 0.216299188 |
| **2** | 28825.7 | 346.9 | 0.310929775 |
| **3** | 31046.9 | 322.1 | 1.187.599.861 |
| **4** | 32206.1 | 310.5 | 0.022443575 |
| **5** | 32867.8 | 304.2 | 0.047409871 |
| **6** | 33903.5 | 295.0 | 0.028226125 |
| **7** | 34251.9 | 292.0 | 0.000966997 |
| **8** | 34921.7 | 286.4 | 0.635586475 |
| **9** | 35690.0 | 280.2 | 0.020108186 |
| **10** | 36099.6 | 277.0 | 0.053597054 |
| **11** | 36325.1 | 275.3 | 0.012563872 |
| **12** | 36898.8 | 271.0 | 0.006741175 |
| **13** | 37367.6 | 267.6 | 0.012238395 |
| **14** | 37586.5 | 266.1 | 0.059165738 |
| **15** | 37764.1 | 264.8 | 0.151384302 |
| **16** | 37860.4 | 264.1 | 0.142868069 |
| **17** | 38071.1 | 262.7 | 0.011419555 |
| **18** | 38272.1 | 261.3 | 0.010665095 |
| **19** | 38301.3 | 261.1 | 0.000468292 |
| **20** | 38601.7 | 259.1 | 0.005996550 |
| **21** | 38880.6 | 257.2 | 0.025543198 |
| **22** | 39340.4 | 254.2 | 0.010505941 |
| **23** | 39404.0 | 253.8 | 0.015936682 |
| **24** | 39595.1 | 252.6 | 0.018947852 |
| **25** | 39806.1 | 251.2 | 0.002517821 |
| **26** | 40487.9 | 247.0 | 0.005281262 |
| **27** | 40637.8 | 246.1 | 0.001911153 |
| **28** | 40918.3 | 244.4 | 0.013556486 |
| **29** | 40932.9 | 244.3 | 0.012341945 |
| **30** | 41608.6 | 240.3 | 0.019794789 |
| **31** | 41747.7 | 239.5 | 0.009042363 |
| **32** | 41879.2 | 238.8 | 0.019012399 |
| **33** | 42286.0 | 236.5 | 0.055273772 |
| **34** | 42335.9 | 236.2 | 0.016950727 |

| | | | |
|---|---|---|---|
| **35** | 42667.0 | 234.4 | 0.090127376 |

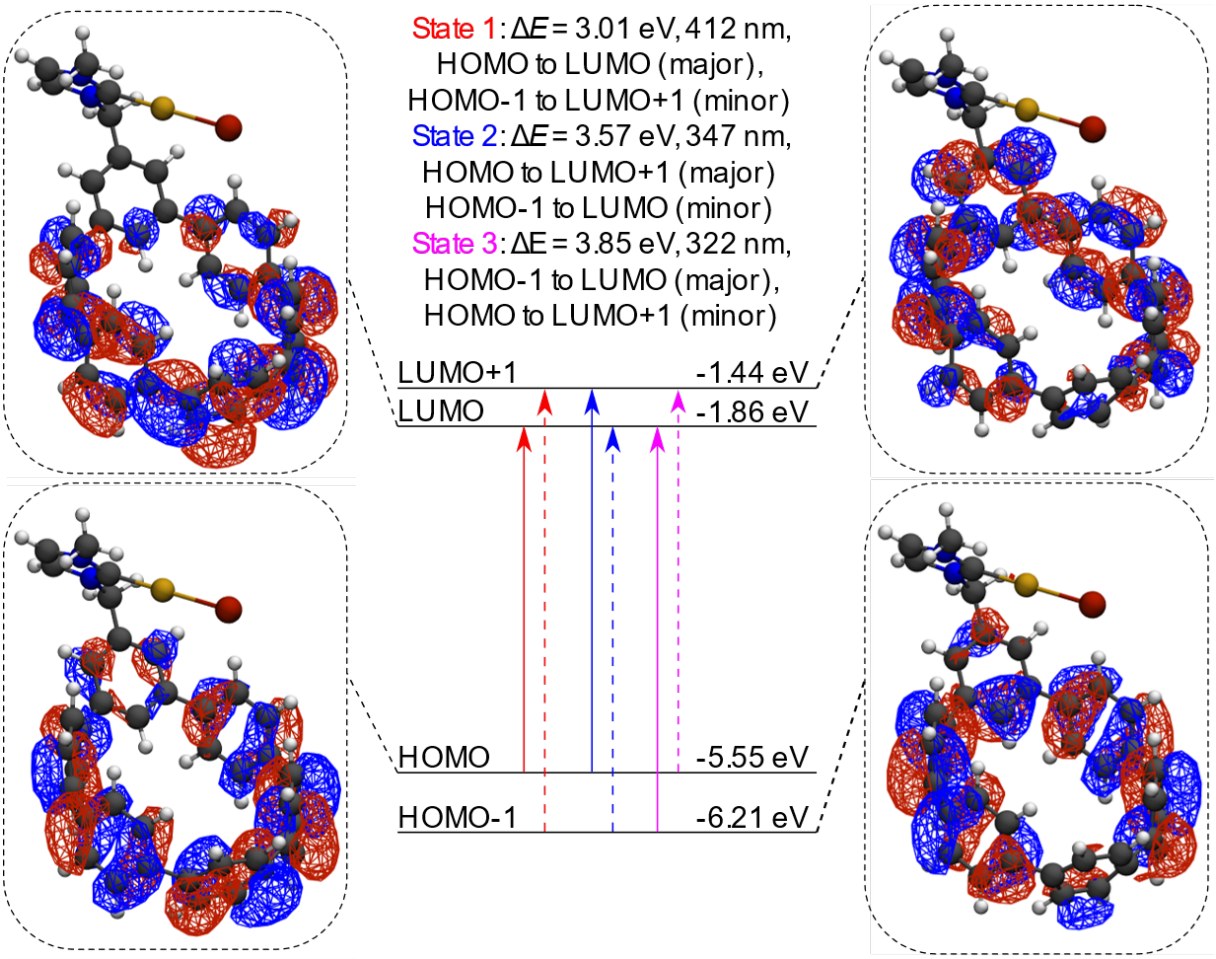


**Figure S8.** Main transitions within the Au(I)-complex **8**, which are visible within the experimental UV/Vis-spectrum and the participating molecular orbitals.

## Generation and results of the steric map using the online-tool SambVCA 2.1:

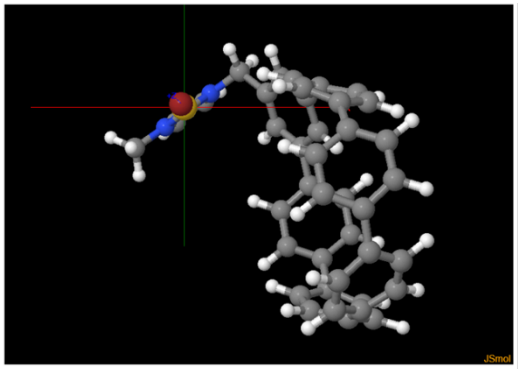


Input completed

submit

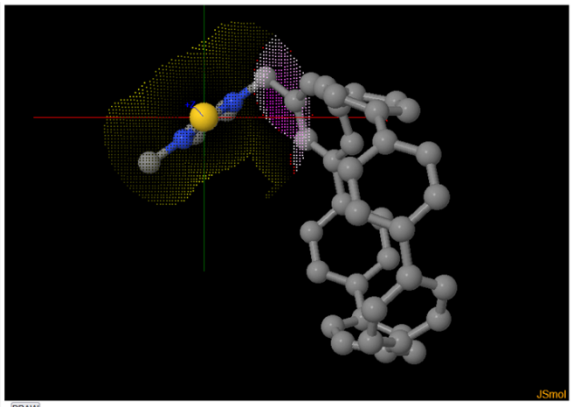


| %V Free | %V Buried | % V Tot/V Ex |
|---|---|---|
| 66.4 | 33.6 | 99.9 |

| Quadrant | V f | V b | V t | %V f | %V b |
|---|---|---|---|---|---|
| SW | 29.8 | 15.1 | 44.9 | 66.4 | 33.6 |
| NW | 36.6 | 8.3 | 44.9 | 81.6 | 18.4 |
| NE | 22.4 | 22.5 | 44.9 | 49.9 | 50.1 |
| SE | 30.4 | 14.5 | 44.9 | 67.7 | 32.3 |

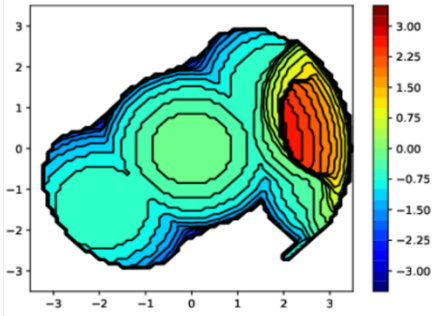


**Figure S9.** Original data from the online-tool SambVCA 2.1 for the theoretically calculated structure of [AuBr(NHC)] complex **8**.

# 6. NMR-Spectra

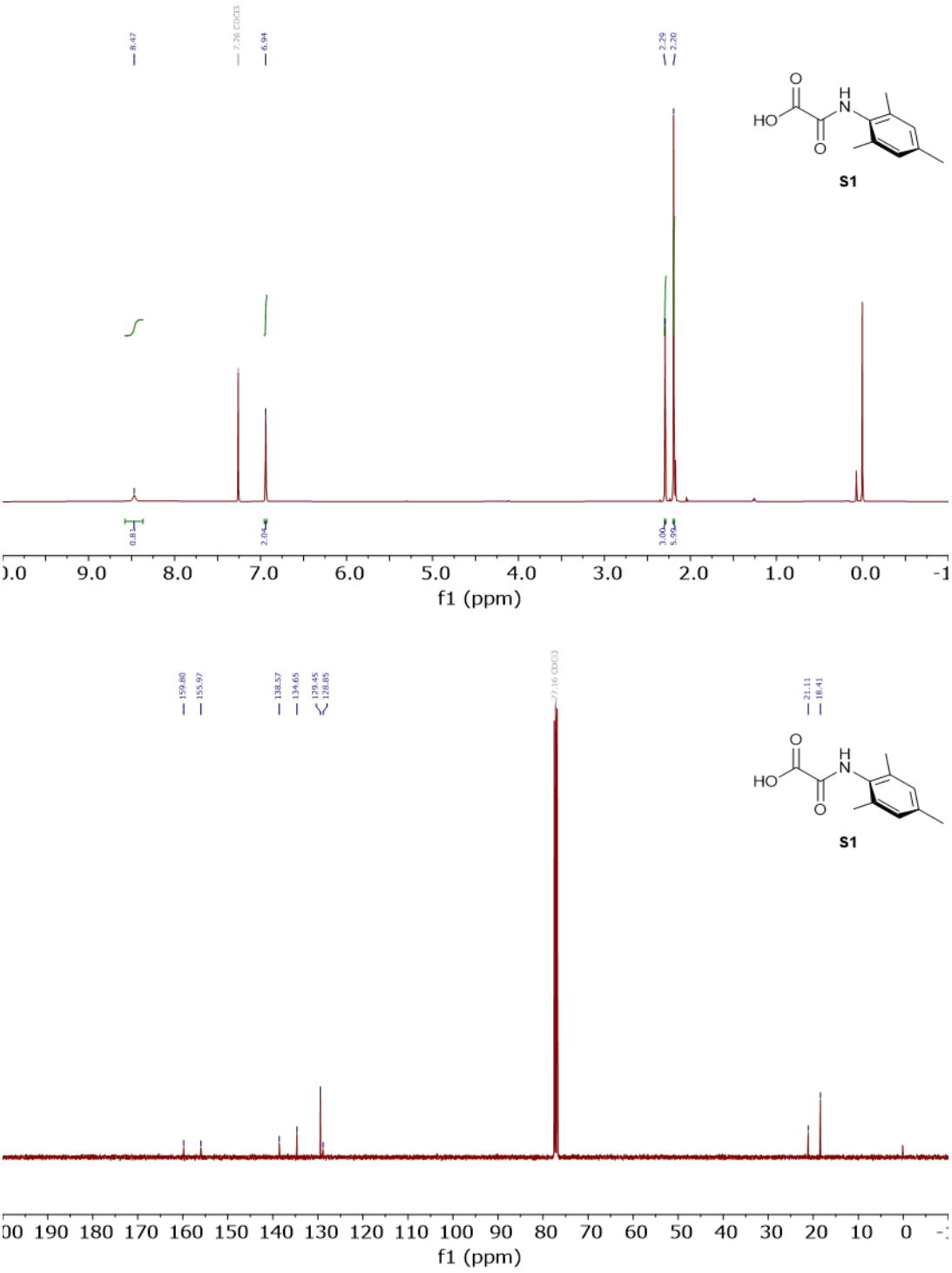


**Figure S10.** $^{1}$H-NMR (top) and $^{13}$C-NMR (bottom) spectra of *N*-(Mesityl)-oxanilic acid **S1** in $CDCl_3$ at rt.

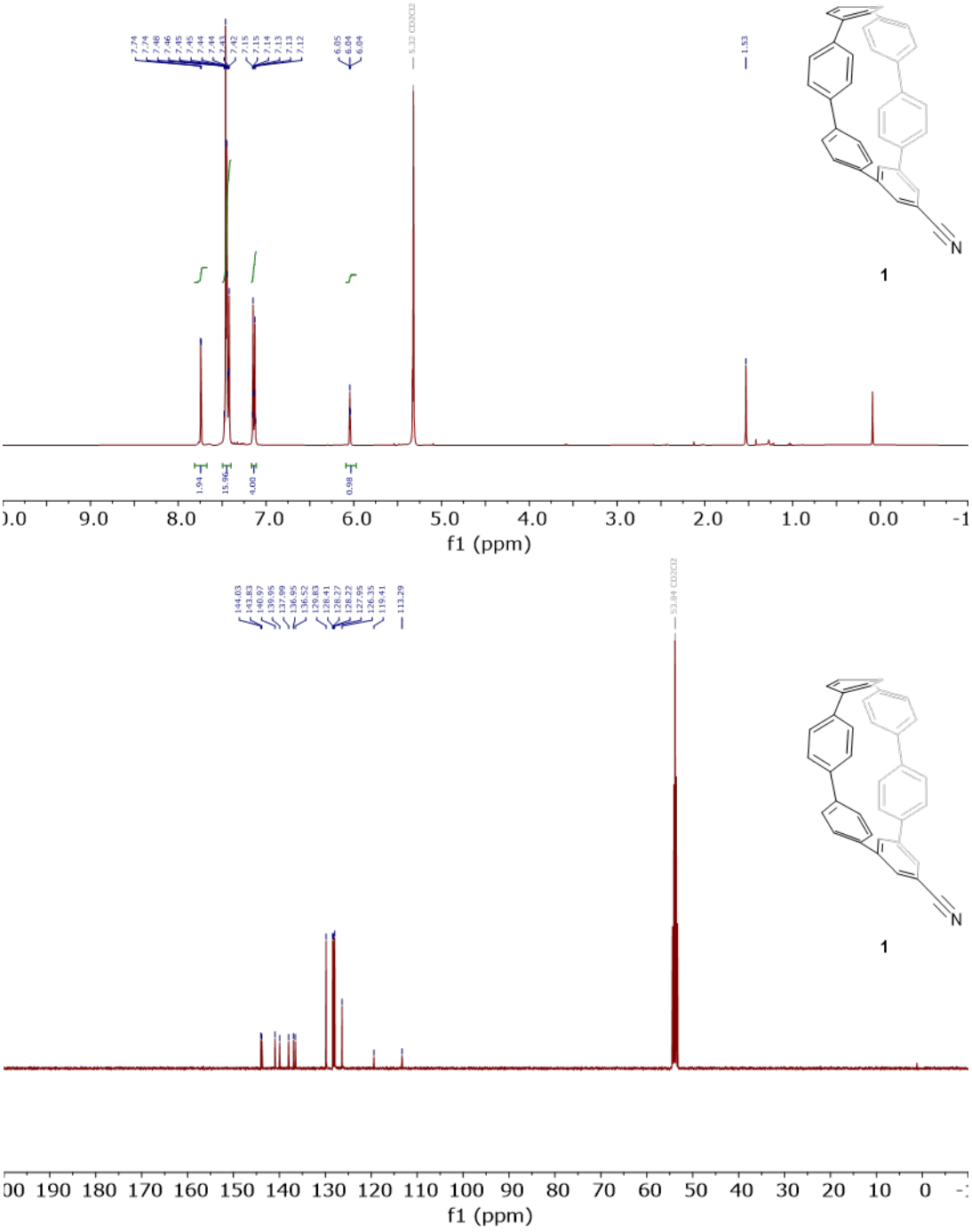


**Figure S11.** $^{1}$H-NMR (top)- and $^{13}$C-NMR (bottom) spectra of cyano-*meta*[6]cycloparaphenylene **1** in DCM-$d_2$ at rt. *Signal at 1.53 ppm corresponds to water occurring from the NMR-solvent.

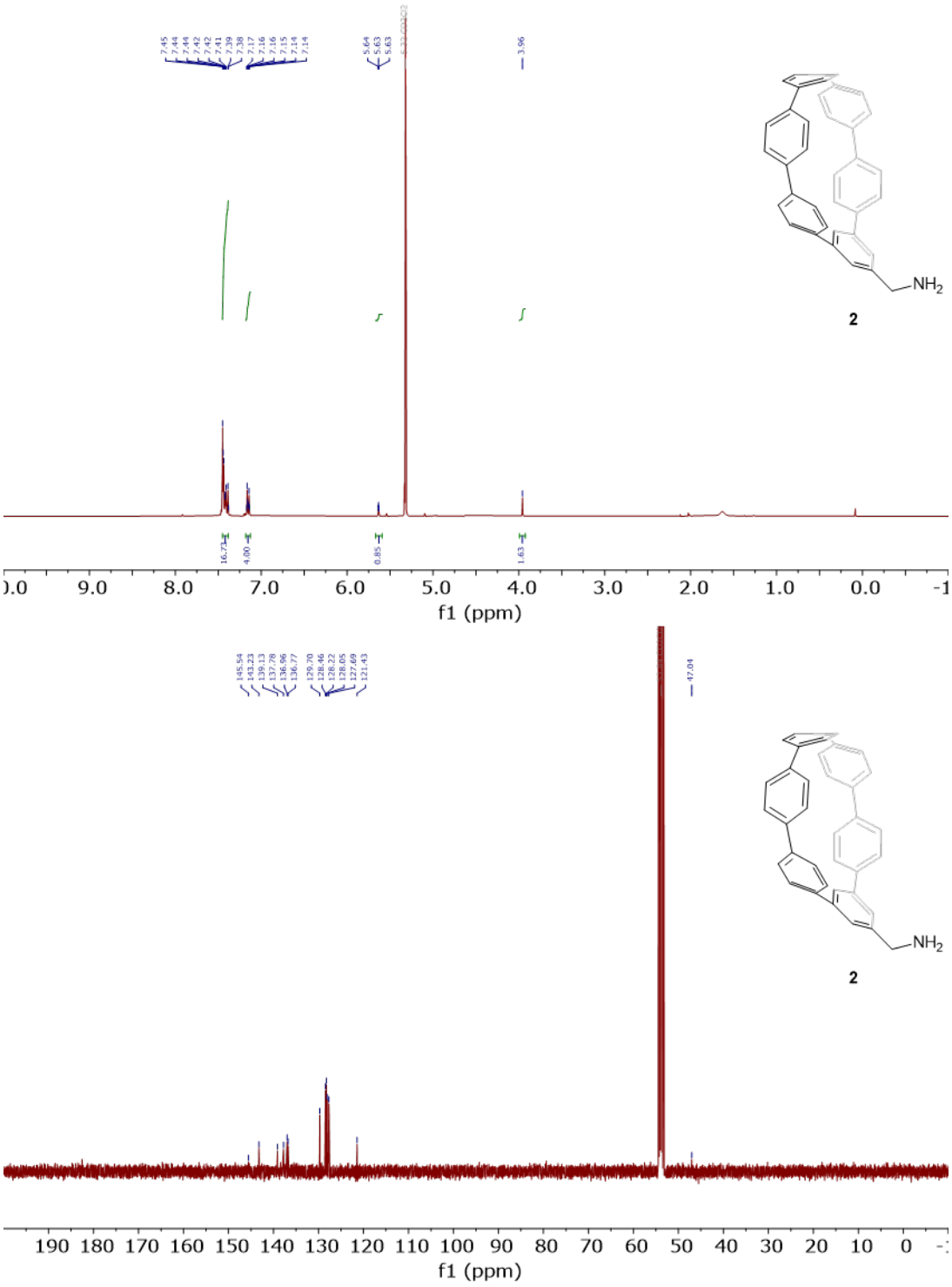


**Figure S12.** $^{1}$H- (top) and $^{13}$C- (bottom) NMR spectra of amino-methylene-*meta*[6]cycloparaphenylene **2** in DCM-$d_2$ at rt. (One carbon signal is missing due to signal to noise ratio).

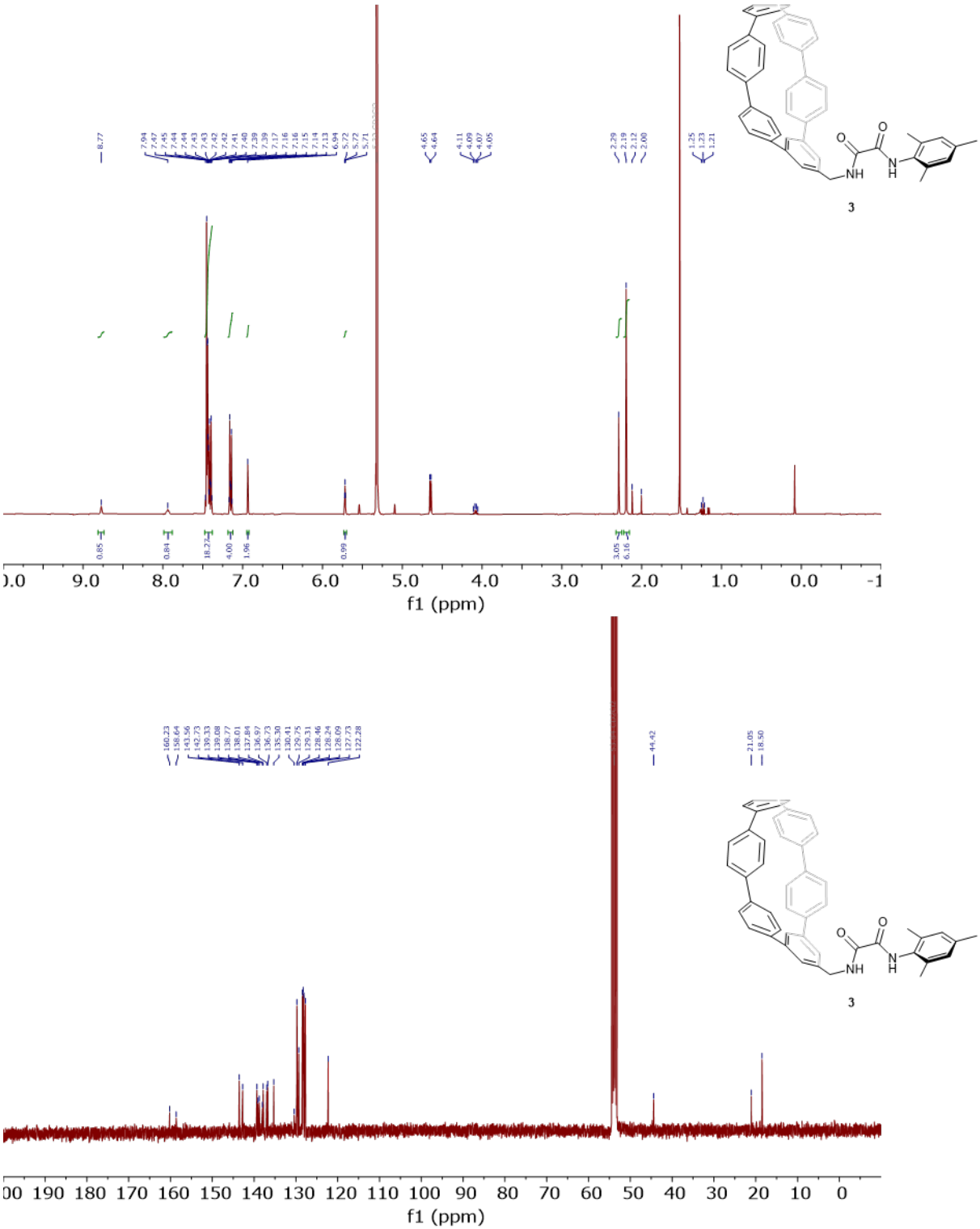


**Figure S13.** $^{1}$H- (top) and $^{13}$C- (bottom) NMR of *N*-(mesityl)-*N'*-(1-methylene-*meta*[6]cycloparaphenylene)oxalamide **3** in DCM-$d_2$ at rt. (Residues of acetone and ethyl acetate in $^{1}$H-NMR spectrum visible.)

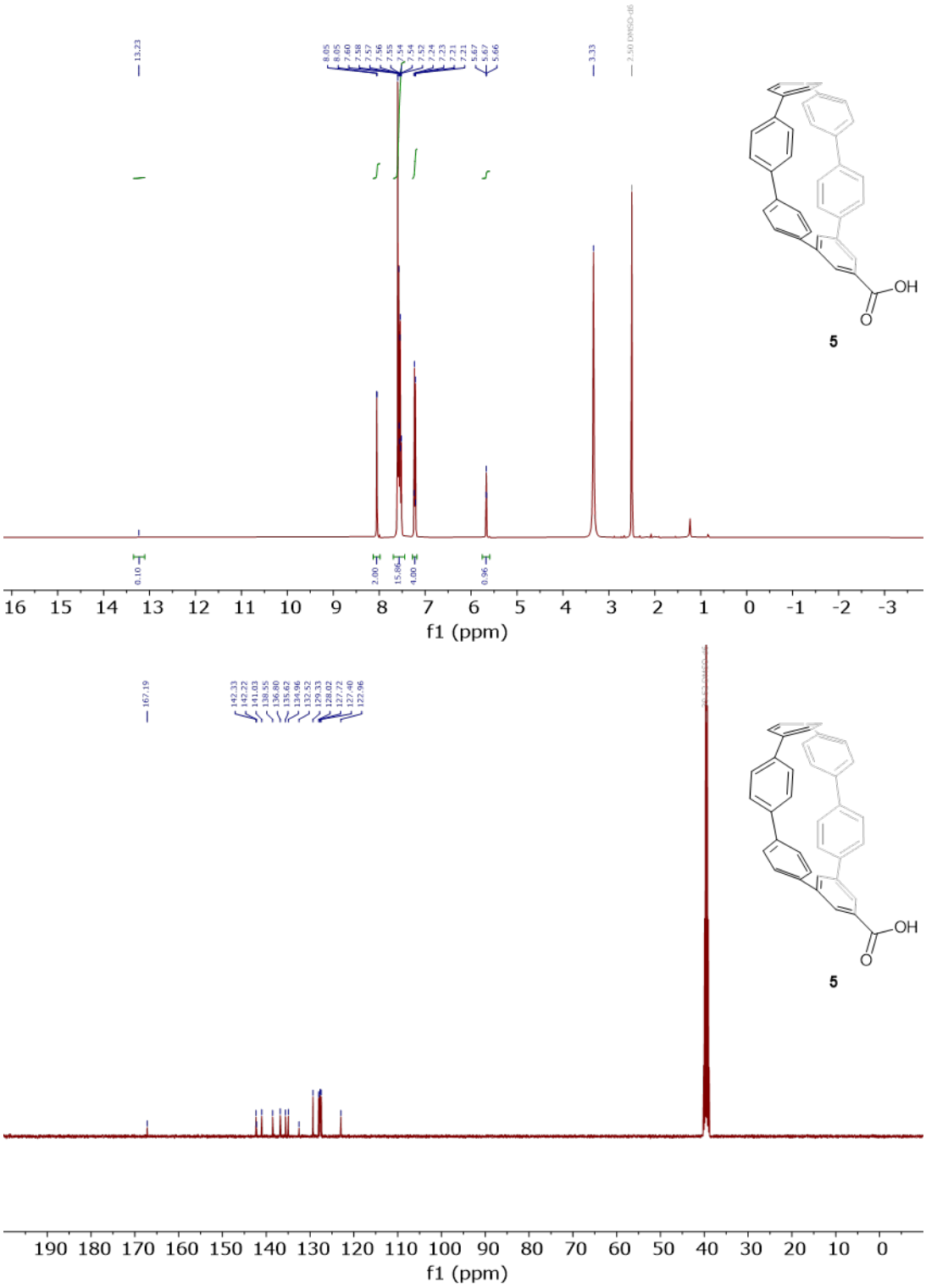


**Figure S14.** $^{1}$H- (top) and $^{13}$C- (bottom) NMR spectra of carboxy-*meta*[6]cycloparaphenylene **5** in DMSO-$d_6$ at rt.

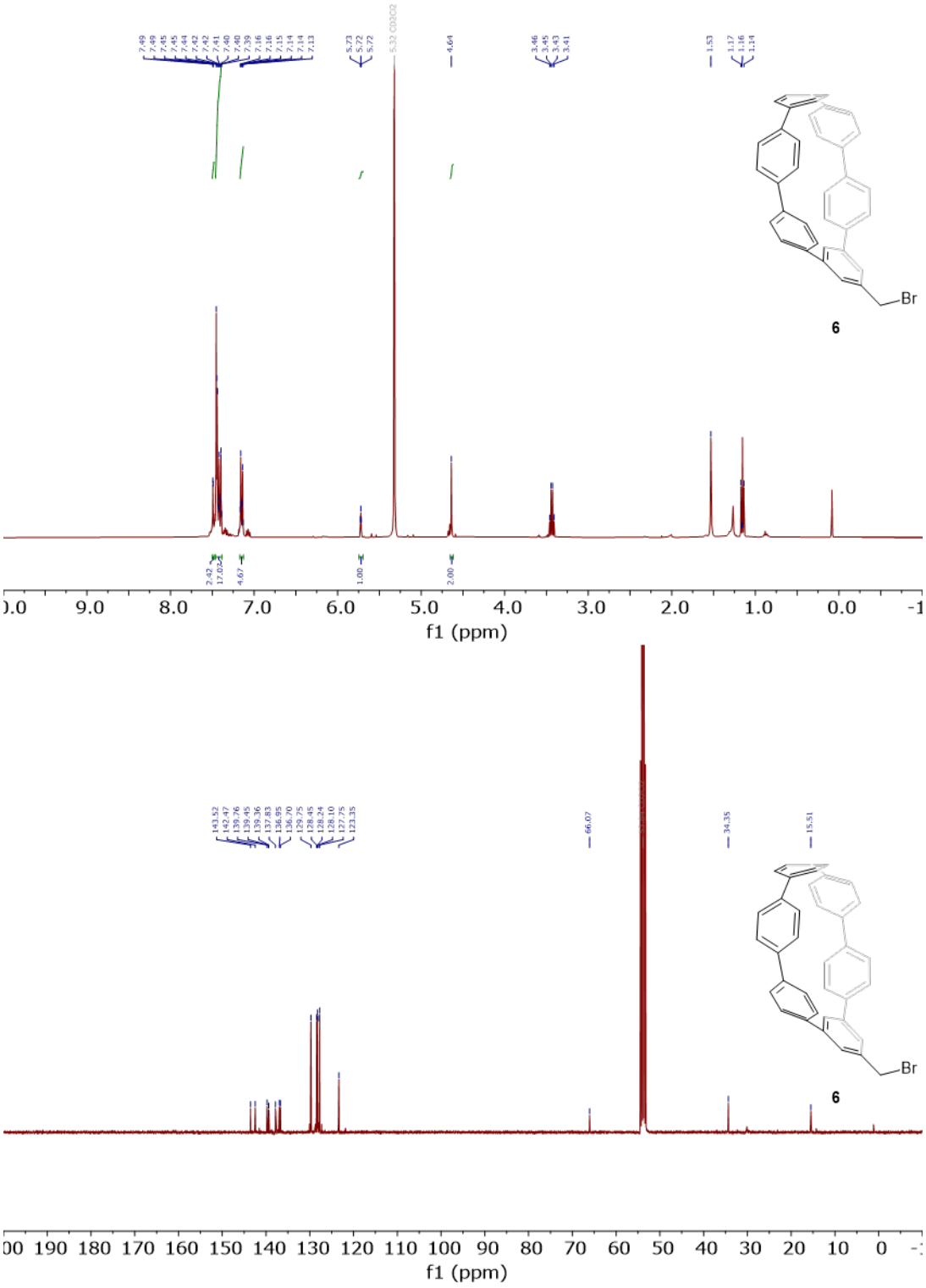


**Figure S15.** $^{1}$H- (top) and $^{13}$C- (bottom) spectra of bromo-methylene-*meta*[6]cycloparaphenylene **6** in DCM-$d_2$ at rt. (Residues of diethyl ether in both spectra visible.)

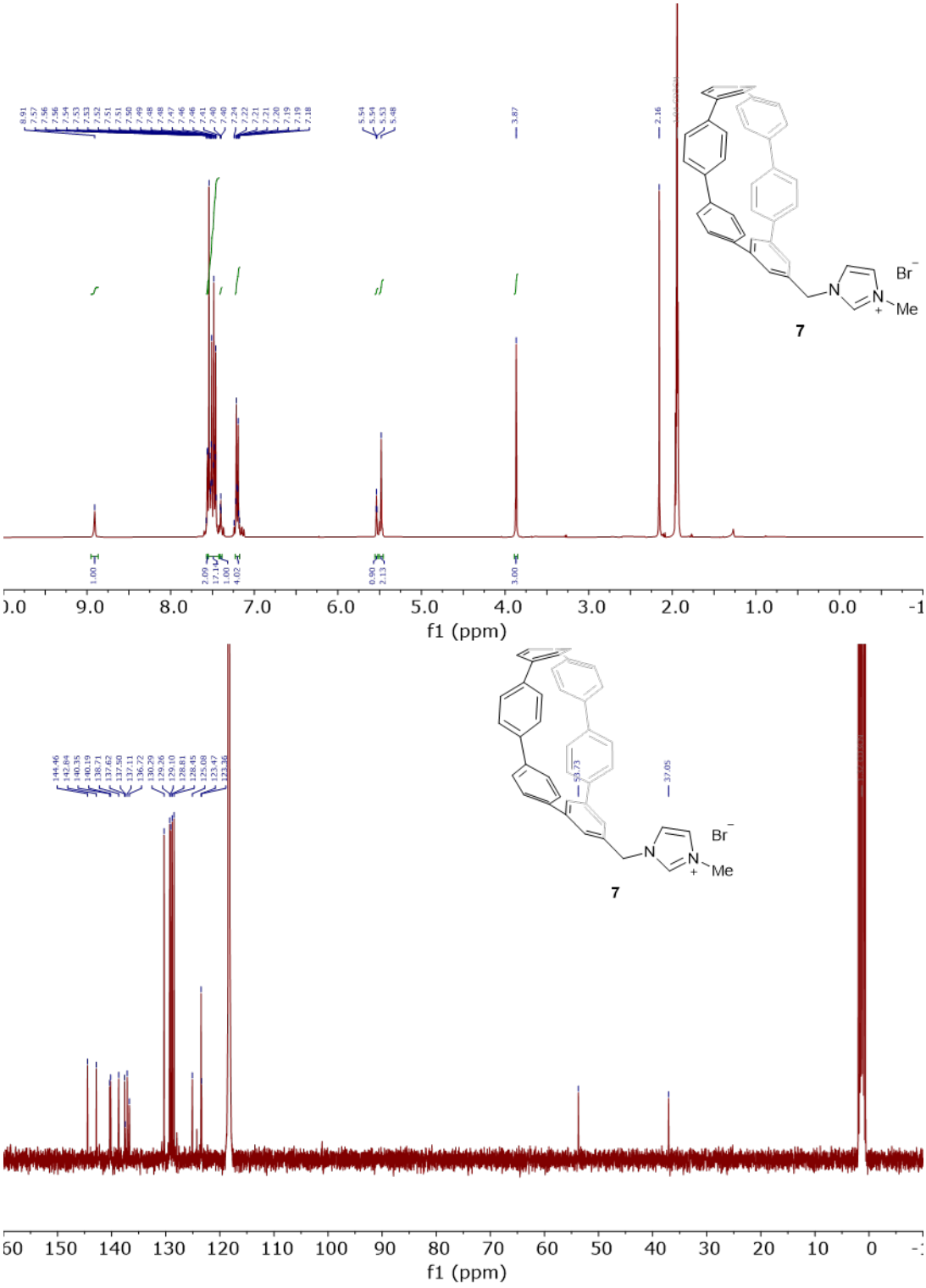


**Figure S16.** $^{1}$H- (top) and $^{13}$C- (bottom) NMR spectra of *N*-(methyl)-*N*'-(1-methylene-*meta*[6]cycloparaphenylene)-imidazolium bromide **7** in MeCN-$d_3$ at rt.

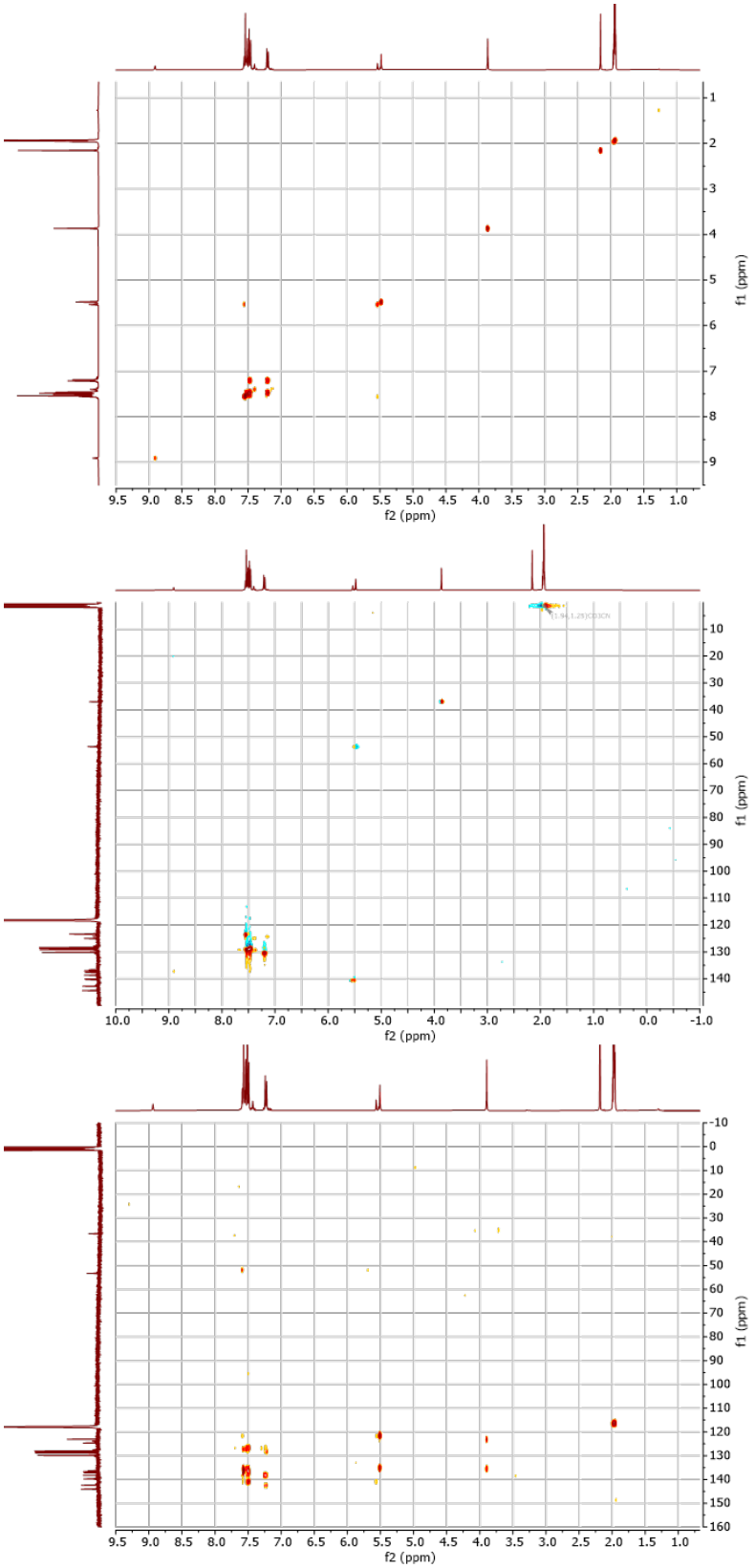


**Figure 17.** $^{1}$H-$^{1}$H-COSY- (top), $^{1}$H-$^{13}$C-HSQC (middle) and $^{1}$H-$^{13}$C- (bottom) NMR spectra of *N*-(methyl)-*N'*-(1-methylene-*meta*[6]cycloparaphenylene)-imidazolium bromide **7** in MeCN-$d_3$ at rt.

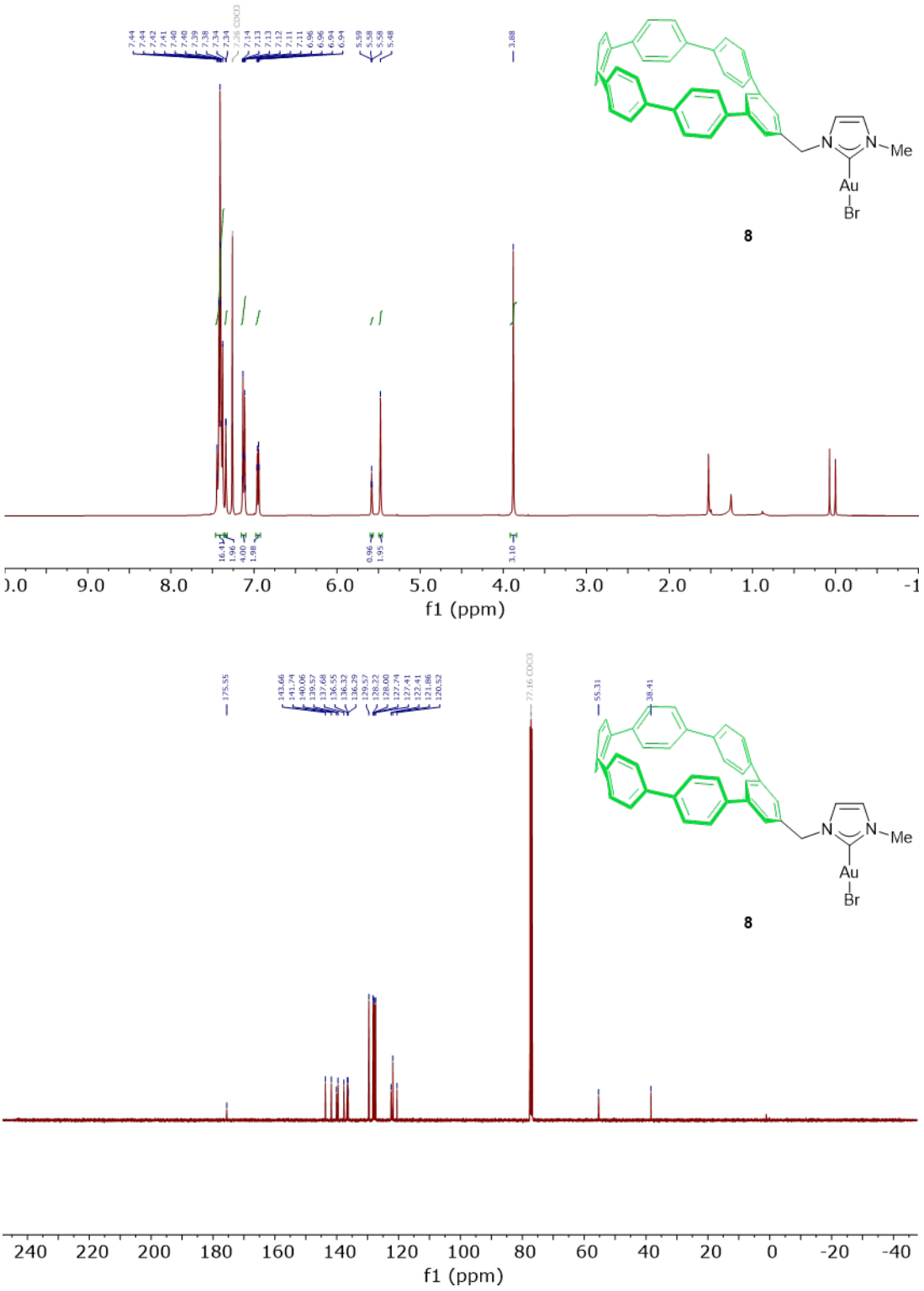


**Figure S18.** $^{1}$H- (top) and $^{13}$C- (bottom) NMR spectra of [*N*-(methyl)-*N'*-(1-methylene-*meta*[6]cycloparaphenylene)-imidazolium]gold bromide **8** in $CDCl_3$ at rt.

# 7. Mass-Spectra of [Au(NHC)Br] 8

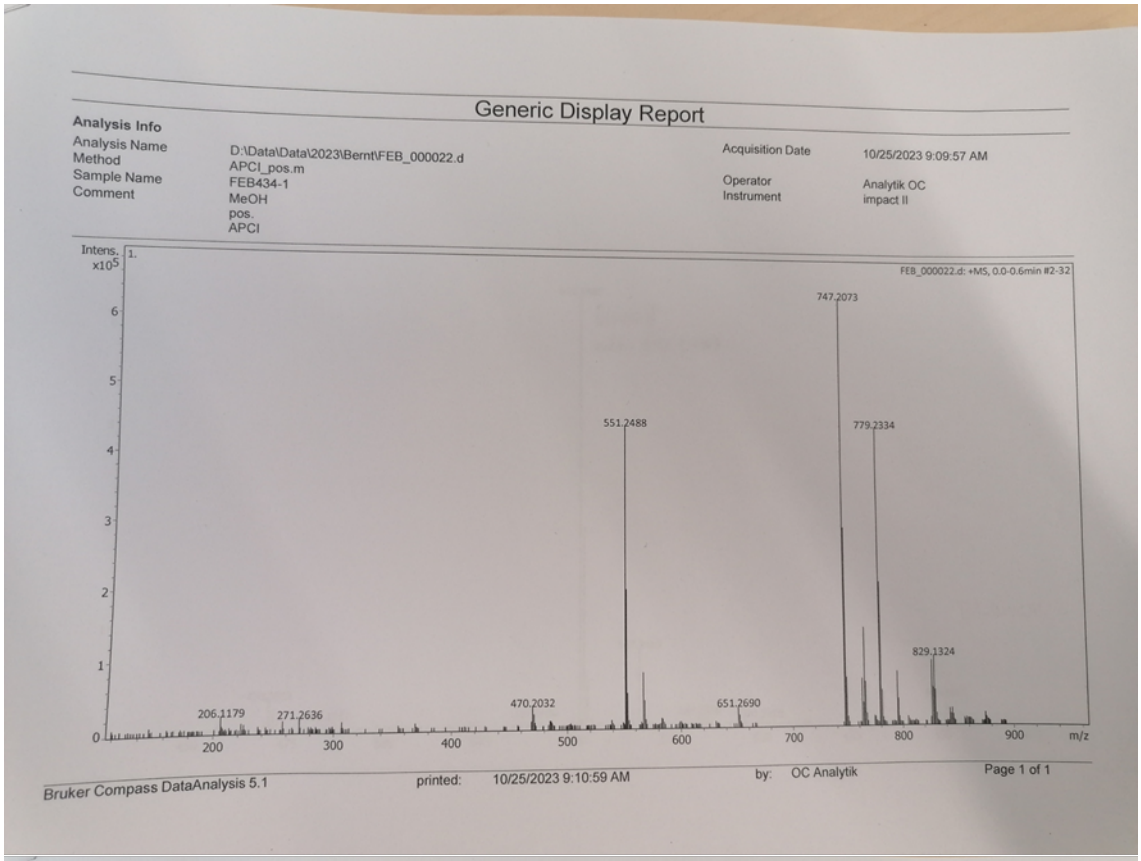


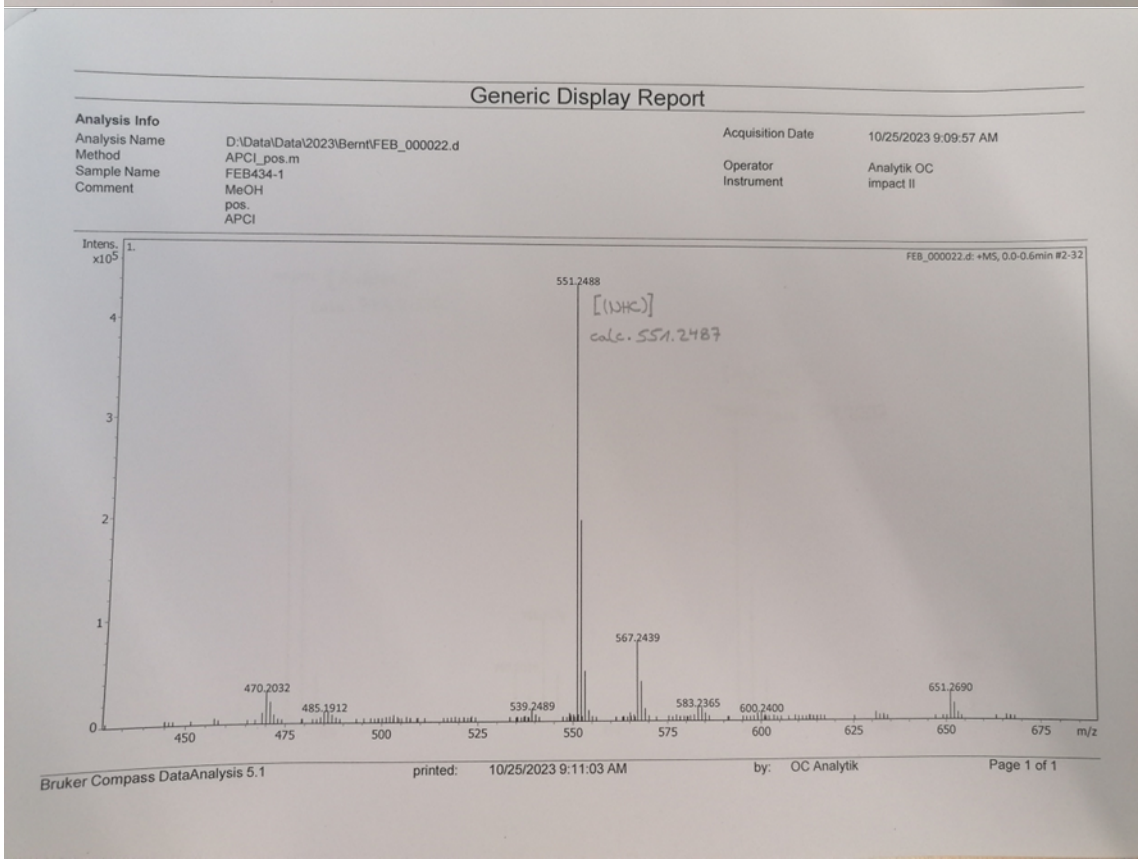

## Generic Display Report

**Analysis Info**

| | | | |
|---|---|---|---|
| Analysis Name | D:\Data\Data\2023\Bernt\FEB_000022.d | Acquisition Date | 10/25/2023 9:09:57 AM |
| Method | APCI_pos.m | | |
| Sample Name | FEB434-1 | Operator | Analytik OC |
| Comment | MeOH<br>pos.<br>APCI | Instrument | impact II |

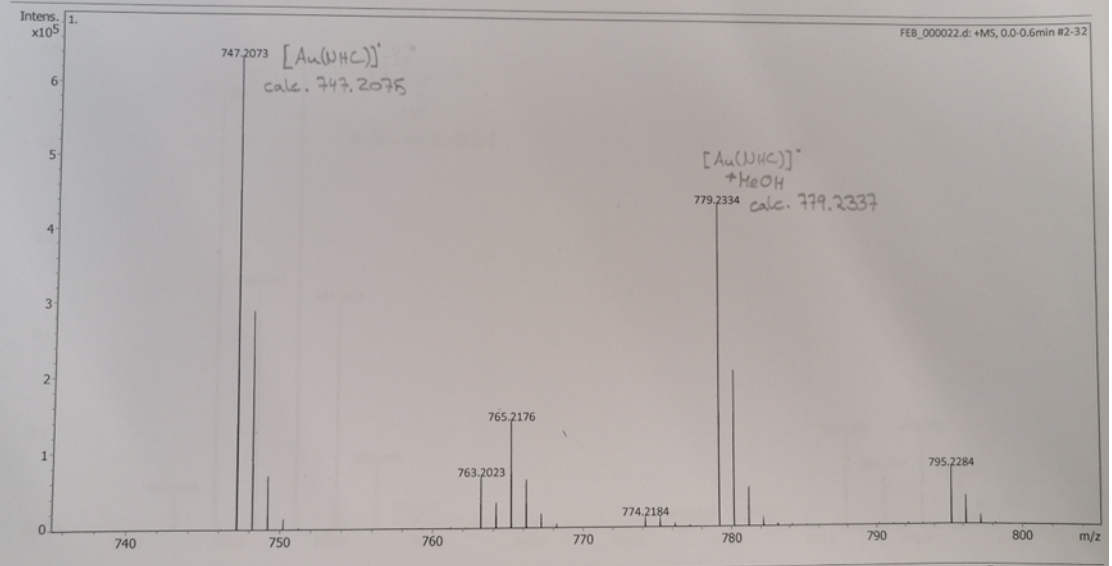


Bruker Compass DataAnalysis 5.1 printed: 10/25/2023 9:11:10 AM by: OC Analytik Page 1 of 1

## Generic Display Report

**Analysis Info**

| | | | |
|---|---|---|---|
| Analysis Name | D:\Data\Data\2023\Bernt\FEB_000022.d | Acquisition Date | 10/25/2023 9:09:57 AM |
| Method | APCI_pos.m | | |
| Sample Name | FEB434-1 | Operator | Analytik OC |
| Comment | MeOH<br>pos.<br>APCI | Instrument | impact II |

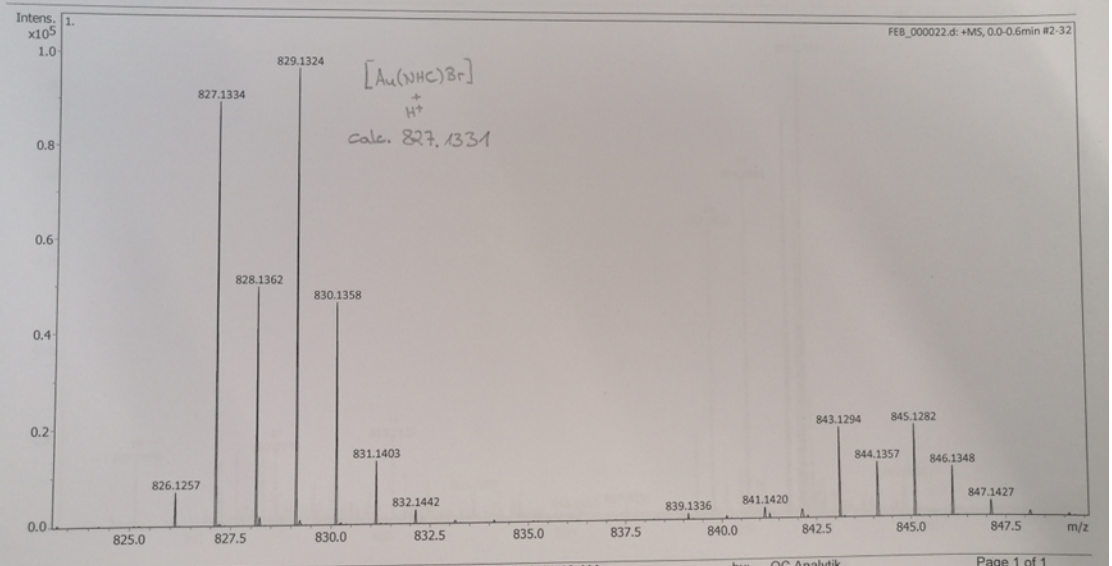


Bruker Compass DataAnalysis 5.1 printed: 10/25/2023 9:11:18 AM by: OC Analytik Page 1 of 1

## 8. ATR-IR Spectrum [AuBr(NHC)] 8

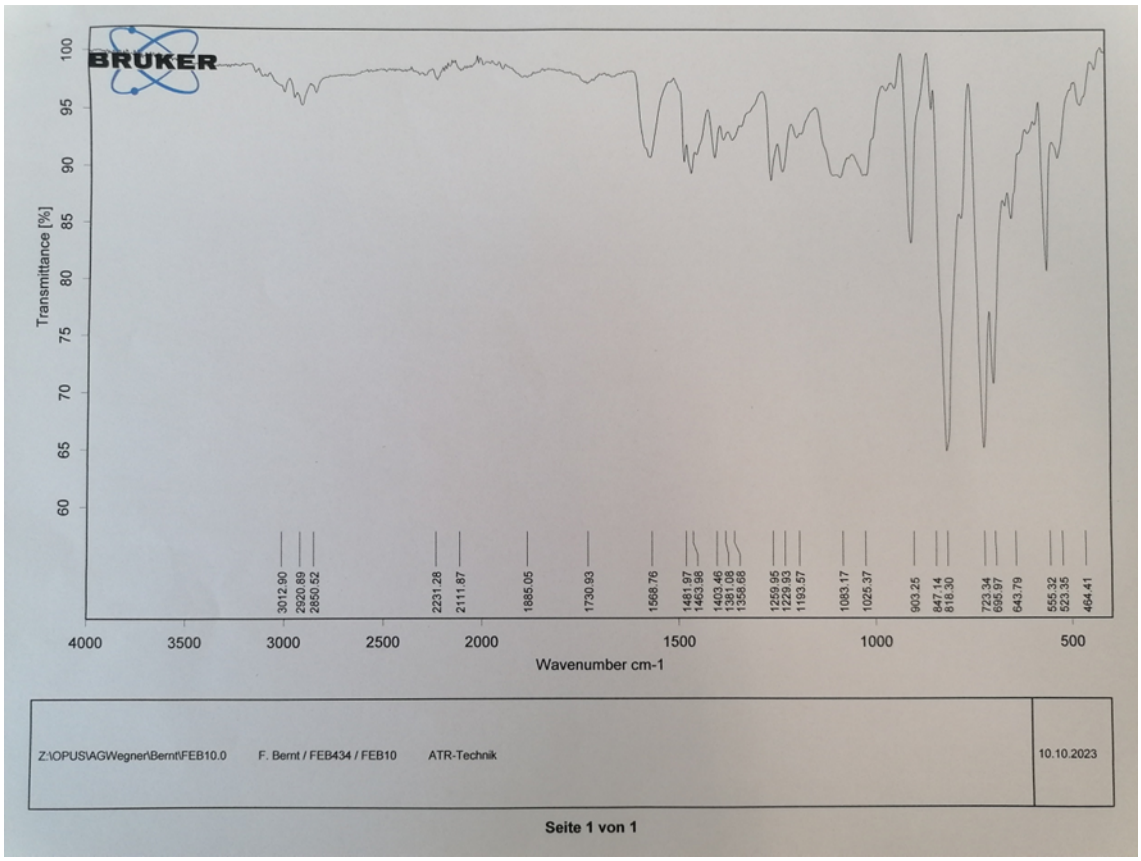

# 9. References


1 L. Krause, R. Herbst-Irmer, G. M. Sheldrick and D. Stalke, *J. Appl. Crystallogr.*, 2015, **48**, 3–10.
2 G. M. Sheldrick, *Acta Crystallogr.*, 2015, **71**, 3–8.
3 G. M. Sheldrick, *Acta Crystallogr.*, 2015, **71**, 3–8.
4 F. Neese, *WIREs Comput. Mol. Sci.*, 2012, **2**, 73–78.
5 F. Neese, *WIREs Comput. Mol. Sci.*, 2022, **12**, e1606.
6 C. Bannwarth, E. Caldeweyher, S. Ehlert, A. Hansen, P. Pracht, J. Seibert, S. Spicher and S. Grimme, *WIREs Comput. Mol. Sci.*, 2021, **11**, e1493.
7 P. Pracht, F. Bohle and S. Grimme, *Phys. Chem. Chem. Phys.*, 2020, **22**, 7169–7192.
8 S. Grimme, *J. Chem. Theory Comput.*, 2019, **15**, 2847–2862.
9 J. P. Perdew, M. Ernzerhof and K. Burke, *J. Chem. Phys.*, 1996, **105**, 9982–9985.
10 C. Adamo and V. Barone, *J. Chem. Phys.*, 1999, **110**, 6158–6170.
11 F. Weigend and R. Ahlrichs, *Phys. Chem. Chem. Phys.*, 2005, **7**, 3297–3305.
12 E. van Lenthe, A. Ehlers and E.-J. Baerends, *J. Chem. Phys.*, 1999, **110**, 8943–8953.
13 S. Grimme, S. Ehrlich and L. Goerigk, *J. Comput. Chem.*, 2011, **32**, 1456–1465.
14 S. Grimme, J. Antony, S. Ehrlich and H. Krieg, *J. Chem. Phys.*, 2010, **132**, 154104.
15 V. Barone and M. Cossi, *J. Phys. Chem. A*, 1998, **102**, 1995–2001.
16 D. A. Pantazis, X.-Y. Chen, C. R. Landis and F. Neese, *J. Chem. Theory Comput.*, 2008, **4**, 908–919.
17 F. Weigend, *Phys. Chem. Chem. Phys.*, 2006, **8**, 1057–1065.
18 B. Helmich-Paris, B. de Souza, F. Neese and R. Izsák, *J. Chem. Phys.*, 2021, **155**, 104109.
19 S. Hirata and M. Head-Gordon, *Chem. Phys. Lett.*, 1999, **314**, 291–299.
20 L. Falivene, Z. Cao, A. Petta, L. Serra, A. Poater, R. Oliva, V. Scarano and L. Cavallo, *Nat. Chem.*, 2019, **11**, 872–879.
21 A. Poater, B. Cosenza, A. Correa, S. Giudice, F. Ragone, V. Scarano and L. Cavallo, *Eur. J. Inorg. Chem.*, 2009, **2009**, 1759–1766.
22 L. Falivene, R. Credendino, A. Poater, A. Petta, L. Serra, R. Oliva, V. Scarano and L. Cavallo, *Organometallics*, 2016, **35**, 2286–2293.
23 A. Poater, F. Ragone, S. Giudice, C. Costabile, R. Dorta, S. P. Nolan and L. Cavallo, *Organometallics*, 2008, **27**, 2679–2681.
24 A. Poater, F. Ragone, R. Mariz, R. Dorta and L. Cavallo, *Chem. Eur. J.*, 2010, **16**, 14348–14353.
25 A. W. Waltman and R. H. Grubbs, *Organometallics*, 2004, **23**, 3105–3107.
26 F. Bernt and H. A. Wegner, *Chem. Eur. J.*, 2023, **29**, e202301001.
27 Recording Fluorescence Quantum Yields, https://static.horiba.com/fileadmin/Horiba/Application/Materials/Material_Research/Quantum_Dots/quantumyieldstrad.pdf.